Cis interactions between CD2 and its ligands on T cells are required for T cell activation

Bin Li, Yan Lu, Ming-Chao Zhong, Jin Qian, Rui Li, Dominique Davidson, Zhenghai Tang, Kaiwen Zhu, Jérémy Argenty, Anne Gonzalez de Peredo, et al.

Cis interactions between CD2 and its ligands on T cells are required for T cell activation

Bin Li1,2, Yan Lu1†, Ming-Chao Zhong1, Jin Qian1, Rui Li1,3, Dominique Davidson1,

Zhenghai Tang1, Kaiwen Zhu1,3, Jérémy Argenty4, Anne Gonzalez de Peredo5,

Bernard Malissen4,6, Romain Roncagalli4, André Veillette1,2,3*

1Laboratory of Molecular Oncology, Institut de recherches cliniques de Montréal (IRCM), Montréal, Québec H2W 1R7, Canada. 2Molecular Biology Program, University of Montréal, Montréal, Québec H3T 1J4, Canada. 3Department of Medicine, McGill University, Montréal, Québec H3G 1Y6, Canada. 4Centre d'Immunologie de Marseille-Luminy, Aix Marseille Université, INSERM, CNRS, 13288 Marseille, France. 5Institut de Pharmacologie et de Biologie Structurale, IPBS, Université de Toulouse, CNRS UPS, Toulouse, France. 6Centre d'Immunophénomique, Aix Marseille Université, INSERM, CNRS, 13288 Marseille, France.

*Corresponding author. Email: andre.veillette@ircm.qc.ca

†Present address: Department of Clinical Immunology, Third Affiliated Hospital of Sun Yat-Sen University, Guangzhou, China.

CD2 is largely described to promote T cell activation when engaged by its ligands, CD48 in mice and CD58 in humans, that are present on antigen-presenting cells (APCs). However, both CD48 and CD58 are also expressed on T cells. By generating new knockout mouse strains lacking CD2 or CD48 in the C57BL/6 background, we deter-mined that whereas CD2 was necessary on T cells for T cell activation, its ligand CD48 was not required on APCs. Rather, CD48 was also needed on T cells. One exception was during cytotoxicity, which required CD48 on T cells and APCs. Fluorescence resonance energy transfer (FRET) studies in nonimmune cells provided evidence that cis interactions between CD2 and CD48 existed within individual cells. CD2-CD48 interactions on T cells enabled more robust T cell receptor (TCR) signals, including protein tyrosine phosphorylation. Using T cells from a CD2 knock-in mouse in which a tag was inserted at the carboxyl terminus of CD2, mass spectrometry analyses revealed that the role of CD2 in T cell activation correlated with its ability to interact with components of the TCR complex and the protein tyrosine kinase Lck. CD2-CD58 provided a similar function in human T cells. Thus, our data imply that T cell–intrinsic cis interactions of CD2 with its ligands are required for TCR signaling and T cell activation. Interactions with ligands on APCs contribute during cytotoxicity.

INTRODUCTION

T cell activation is a critical component of antigen-specific immunity needed for protection against microbial pathogens and tumor cells (1–3). It is implicated in the pathophysiology of autoimmune diseases such as diabetes and rheumatoid arthritis. For T cells to respond ade-quately to antigens, multiple receptors, activating or inhibitory, recog-nize ligands that may or may not be expressed on antigen- presenting cells (APCs). Chief among them is the T cell receptor (TCR), which recognizes antigens associated with major histocompatibility complex (MHC) molecules on APCs. T cells also

express coreceptors (namely, CD4 and CD8), costimulatory receptors (including CD28 and ICOS), and coinhibitory receptors (like PD-1 and CTLA-4), which can also be triggered by ligands on APCs to modulate T cell activation.

CD2 is a transmembrane immunoglobulin (Ig) superfamily member broadly expressed on T cells and natural killer (NK) cells (4–6). It is distantly related to the SLAM family of receptors (7). CD2 recognizes as ligands CD48 (in mice) and CD58 (also known as LFA-3; in humans), two glycosylphosphatidylinositol (GPI)–linked recep-tors expressed on APCs. CD48 is expressed on all T cells in mice at levels analogous to those seen in APCs such as dendritic cells and macro-phages (www.immgen.org). CD58 is highly expressed in effector- memory and innate-like T cells in humans, in amounts also analogous to those seen in APCs (www.immgen.org/Databrowser19/Human-ExpressionData.html). Imaging analyses using CD58 immobilized on artificial lipid bilayers suggested that, upon engagement by ligands on APCs (hereafter termed "trans" interactions), CD2 becomes part of the T cell "immunological synapse" (8–10). As stimulation of T cells with agonistic anti-CD2 antibodies (Abs) resulted in markedly enhanced T cell activation, it has been implied that CD2 is a potent T cell–activating receptor (4–6). Conversely, it was also shown that blocking anti-CD2 Abs diminished T cell activation, leading to the idea that CD2 blockade may be useful for the treatment of T cell–mediated diseases such as graft rejection and autoimmunity in humans (11).

Genetic studies have provided more conflicting evidence on the importance of CD2 in T cell activation. Initial analyses of genetically engineered CD2-deficient [knockout (KO)] mice on a mixed genetic background [129-C57BL/6 (B6)] suggested that these animals had normal T cell responses (12). However, a subsequent study showed reduced responses to low-affinity, but not high-affinity, antigenic peptides (13, 14). Another study found that the CD2 KO mice dis-played normal or only minimally compromised T cell responses to anti-CD3 Abs or antigenic peptides, although CD2 deficiency ac-centuated the defects caused by lack of CD28 (15).

Although CD2 has been presumed to be engaged by ligands dis-played on APCs (8, 9), these ligands are also expressed on T cells, suggesting that interactions within individual T cells or between adjacent T cells (hereafter termed "cisT" and "cisT-T" interactions, respectively) may also exist. Some evidence in support of this idea was reported by others (4, 16, 17), although the prevalent view is still that CD2 is engaged by ligands from APCs. To address this matter, we analyzed T cell functions in newly generated mouse strains lacking CD2 or CD48 in a pure B6 background. We found that T cells lacking CD2 had broad activation defects in vitro and in vivo. Unexpectedly, identical defects were seen in T cells lacking CD48. Only CD2-dependent cytotoxicity necessitated CD48 on APCs. Imaging analyses provided evidence that CD2 and CD48 interacted in cis at the surface of individual T cells. Biochemical studies indicated that these interactions boosted TCR signaling, an impact correlating with the ability of CD2 to recruit the kinase Lck. A similar function was documented for CD2-CD58 interactions in human T cells. Therefore, cis interactions between CD2 and its ligands in T cells are required for TCR signaling and T cell activation. Although CD2 can also respond to ligands displayed on APCs, these trans inter-actions are critical in more limited settings such as cytotoxicity.

RESULTS

Lack of CD2 broadly compromises T cell responses even in the absence of APCs

To address the role and triggering mechanism of CD2 in T cells, we generated new CD2 KO mouse strains in the pure C57BL/6 back-ground. Compared with control wild-type (WT) mice, CD2 KO mice lacked CD2 but had normal expression of other T cell markers, including TCR and CD3, in thymus and

spleen (fig. S1, A and B). They also had normal T cell subsets in spleen, with normal propor-tions and numbers of regulatory, naïve, effector-memory, and cen-tral memory T cells (fig. S1, C and D).

To test T cell activation in vitro, freshly isolated T cells from CD2 KO mice were stimulated with various stimuli requiring or not requiring APCs. Compared with WT T cells, CD2 KO T cells, either CD4+ or CD8+, displayed reduced proliferation (as measured by thymidine incorporation) and production of cytokines [interleukin-2 (IL-2), interferon-g (IFN-g), and IL-4], in response to anti-CD3 Abs, in the absence or presence of anti-CD28 Abs (Fig. 1A). Similar defects were observed with the lectin concanavalin A (Con A; "C") but not with the combination of phorbol 12-myristate 13-acetate (PMA) and ionomycin (P + I), which bypasses the proximal TCR signaling apparatus (Fig. 1B). Analogous activation defects were noted when WT T cells were treated with blocking anti-CD2 Ab RM2-5 compared with isotype control Ab (Fig. 1C).

In response to irradiated WT splenocytes as APCs plus the super-antigen staphylococcal enterotoxin B (SEB), CD2 KO CD4+ T cells also had a pronounced deficiency in T cell activation when com-pared with WT CD4+ T cells (fig. S1E). SEB activates CD4+ T cells expressing Vb8.1 or Vb8.2 (18). These T cell subsets were present in equal proportions in CD2 KO and WT mice (fig. S1F). Likewise, in response to irradiated splenocytes from WT BALB/c mice, CD2 KO CD8+ T cells showed a marked activation defect compared with WT CD8+ T cells (fig. S1G). This "alloreactive response" occurs because TCRs from C57BL/6 mice recognize mismatched class I MHC from BALB/c mice as alloantigen.

To analyze antigen-specific responses, we also bred CD2 KO mice with OT-I or OT-II mice, which express a transgenic TCR reactive against ovalbumin (OVA) presented by class I or class II MHC, respectively. When activated by irradiated WT splenocytes and the high-affinity agonistic OVA peptide N4 (SIINFEKL), freshly isolated CD2 KO OT-I CD8+ T cells displayed a severe decrease (up to 90%) in proliferation and cytokine secretion in comparison with WT OT-I CD8+ T cells (Fig. 1D). A more pronounced defect was noted with the low-affinity agonistic peptide G4 (SIIGFEKL) (Fig. 1E). An analogous defect was noted when CD2 KO OT-II CD4+ T cells were activated with irradiated WT splenocytes and the OVA peptide OVA323–339, compared with WT OT-II CD4+ T cells (Fig. 1F).

Hence, T cells from CD2 KO mice, both CD4+ and CD8+, displayed pronounced activation defects in response to multiple stimuli in the absence or presence of APCs. Analogous deficits were caused by addition of a blocking anti-CD2 Ab.

CD2 on T cells is engaged by CD48 on T cells

The observation that CD2 was critical for T cell activation even in the absence of APCs implied that CD2 was engaged by ligands present on T cells. The only known ligand of CD2 in mice is CD48. To examine whether other ligands may exist for CD2, we first performed binding assays using a soluble Fc fusion protein encompassing the extracellu-lar domain of CD2 and purified T cells from WT, CD48 KO, or CD2 KO mice. Using the CD2-Fc fusion protein (hereafter termed CD2-Fc) as probe, specific staining was noted on WT T cells (Fig. 2A). This staining was completely abolished on CD48 KO T cells. Binding was greater (~3.5-fold) when CD2 KO T cells were used for staining. This difference was not due to increased CD48 expression on CD2 KO T cells, as shown by the calculated mean fluorescence intensity (MFI) ratio of CD2-Fc over CD48 (fig. S2A).

In a similar way, when a CD48-Fc fusion protein was used as probe, specific staining was seen on WT T cells, but not on CD2 KO T cells (Fig. 2A). Moreover, staining was greater (~3-fold) on CD48 KO T cells compared with WT T cells, and this increase was not caused by greater CD2 expression (Fig. 2A and fig.

S2A). No expression of 2B4, another receptor capable of binding CD48 and encoded by the Cd244 gene (4), was noted on these cells (Fig. 2A). This was true whether cells were activated or not (Fig. 2B). In mice, 2B4 is expressed on intraepithelial lymphocytes, some gd T cells and exhausted T cells, but not on most other T cells (www.immgen.org).

To address whether CD2 and CD48 were interacting with each other at the surface of individual T cells, their colocalization was ascertained by confocal microscopy. Using fluorescence-coupled Abs, we observed that substantial proportions of CD2 and CD48 were colocalized at the surface of individual T cells (Fig. 2C). No colocaliza-tion of the fluorochromes was seen with CD2 KO or CD48 KO T cells.

We also examined the ability of CD2 and CD48 to interact in cis using fluorescence resonance energy transfer (FRET) coupled with confocal microscopy. To this end, constructs encoding SNAP-tagged CD2 and CLIP-tagged CD48 were cotransfected into human embryonic kidney (HEK) 293T cells. After labeling the tags with an energy acceptor [Alexa Fluor 647 (AF 647)] or an energy donor [Dyomics 547 (DY 547)], respectively, photobleaching of the acceptor was performed (Fig. 2D). Then, the impact of photobleaching on the fluorescence of CD48-coupled 547 was measured. Photobleaching resulted in a pronounced increase (~30%) in the fluorescence of CD48-coupled 547 (Fig. 2D). This effect was markedly attenuated (reduced to ~10%) by addition of blocking anti-CD2 Ab RM2-5 compared with control Ab. The recovery of donor fluorescence after acceptor photobleaching implied that CD2 and CD48 were in close proximity at the cell surface.

Thus, CD2 and CD48 were an exclusive receptor-ligand pair and interacted in cis at the surface of individual T cells. In T cells lacking either molecule, the remaining component of the pair showed an increased capacity to recognize an exogenous fusion protein corre-sponding to the missing molecule, suggesting that the absence of cis interactions may facilitate trans interactions.

CD48 KO T cells phenocopy the functional defects of CD2 KO T cells

If the cis interactions between CD2 and CD48 were critical for T cell activation, one would expect that CD48 KO T cells might display identical activation defects compared with CD2 KO T cells. No defect in

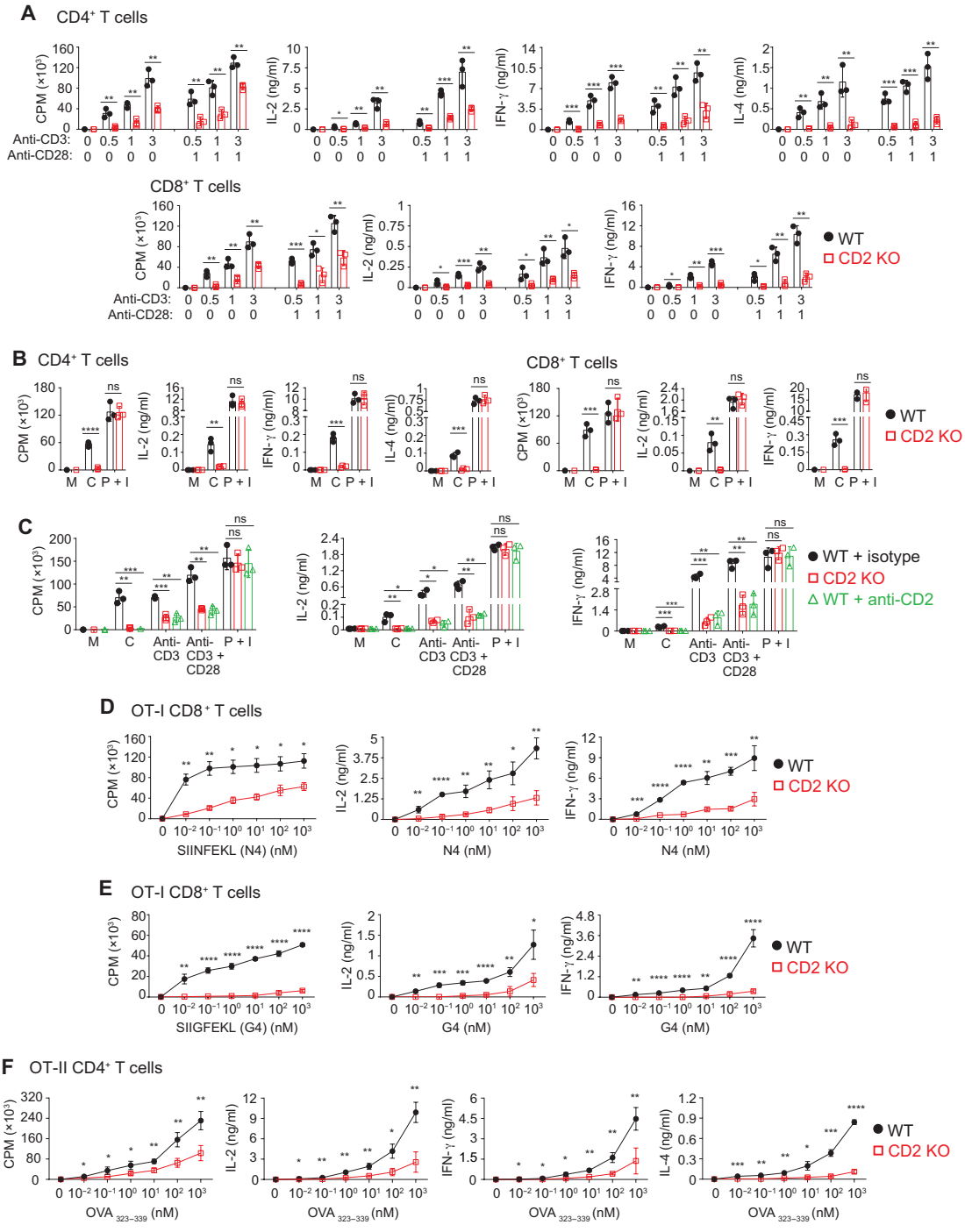

Fig. 1. Loss of CD2 in T cells broadly compromises T cell activation. (**A**) Freshly isolated $CD4^+$ splenic T cells [depleted of invariant natural killer T (iNKT) cells] or $CD8^+$ splenic T cells (10^6 cells ml^{-1}) from WT or CD2 KO mice were stimulated with the indicated concentrations of anti-CD3 Abs (0, 0.5, 1, and 3 μg ml^{-1}) without or with anti-CD28 Abs (1 μg ml^{-1}). After 48 hours, proliferation was assessed by measuring thymidine incorporation [in counts per minute (cpm)], whereas cytokine production was determined by ELISA. (**B**) Same as (A), except that cells were stimulated with Con A ("C"; 4 μg ml^{-1}) or PMA (100 ng ml^{-1}) plus ionomycin (1 μg ml^{-1}) (P + I). M, culture medium alone. (**C**) As in (A), except that blocking anti-CD2 Ab RM2-5 or isotype-matched rat IgG2b (1 μg ml^{-1}, coated on plastic) was also added during stimulation of freshly isolated $CD8^+$ splenic T cells. (**D** and **E**) Freshly isolated $CD8^+$ splenic T cells (10^6 cells ml^{-1}) from WT or CD2 KO mice bred with class I MHC–restricted TCR transgenic (Tg) mouse OT-I were activated with the indicated concentrations of high-affinity agonistic OVA amino acid 257–264 peptide N4 (SIINFEKL) (D) or low-affinity agonistic OVA peptide G4 (SIIGFEKL) (E) plus irradiated C57BL/6 splenocytes as APCs. After 24 hours, activation was monitored as detailed in (A). (**F**) Freshly isolated $CD4^+$ splenic T cells from WT or CD2 KO mice bred with class II MHC–restricted TCR transgenic (Tg) mouse OT-II were activated with the indicated concentrations of OVA peptide $OVA_{323–339}$ plus irradiated C57BL/6 splenocytes as APCs. Activation was monitored as detailed in (A). Each symbol in (A) to (C) represents an individual mouse; results are pooled from three independent experiments with a total of three mice in (A) to (F). Error bars represent means with SD. $^*P \leq 0.05$, $^{**}P \leq 0.01$, $^{***}P \leq 0.001$, $^{****}P \leq 0.0001$, not significant (ns) $P > 0.05$ (two-sided unpaired Student's *t* tests).

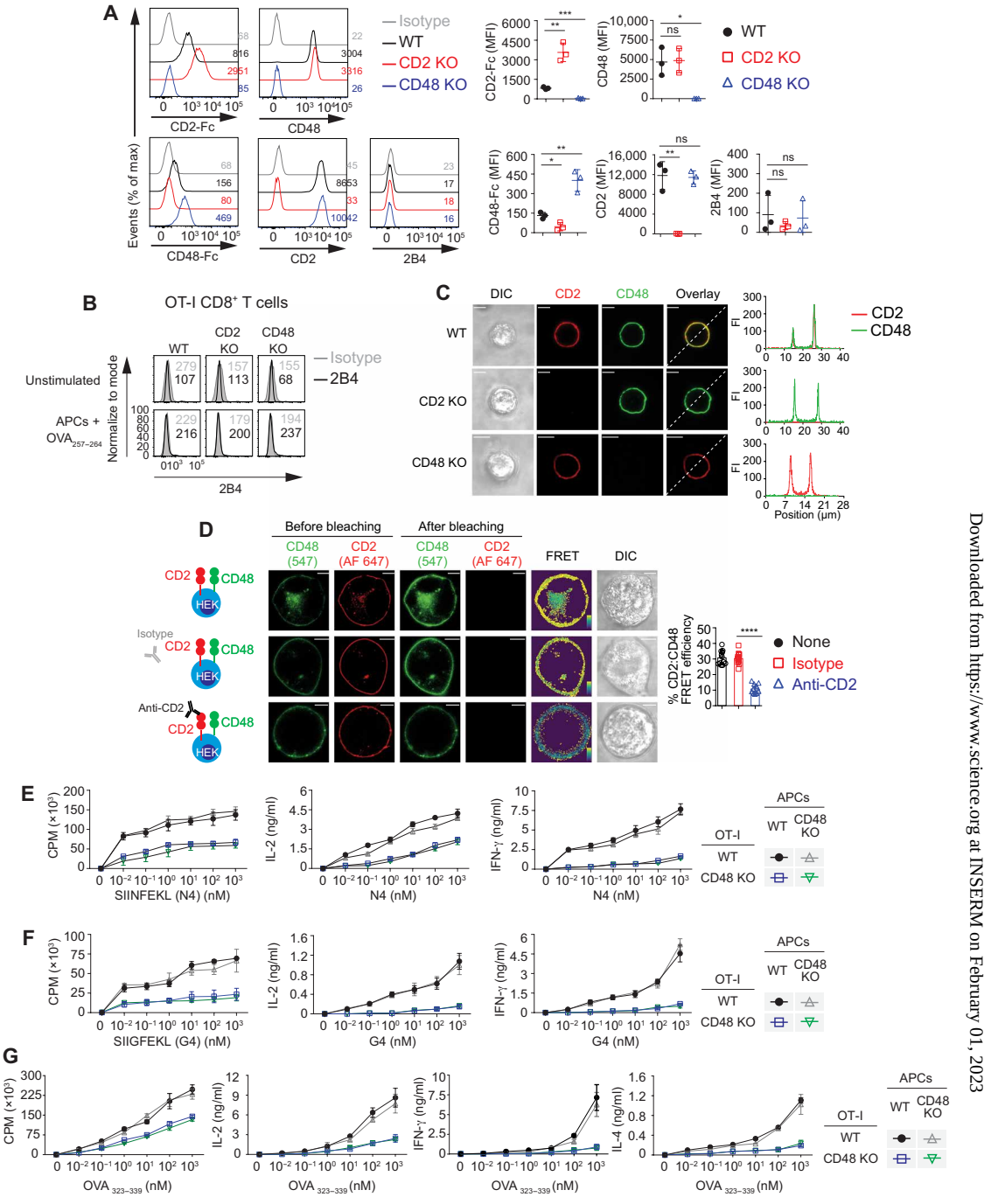

Fig. 2. CD2 interacts with its ligand CD48 in cis to promote T cell activation. (**A**) Freshly isolated OT-II CD4$^+$ splenic T cells from WT, CD2 KO, and CD48 KO mice were activated with peptide + APCs and stained with Fc fusion proteins encompassing the extracellular domain of CD2 or CD48, followed by a secondary Ab directed against the Fc segment of the fusion proteins. Expression of CD2, CD48, and 2B4 was analyzed in parallel by staining cells with Abs directed against these molecules. Controls were WT cells stained with isotype control IgG (isotype). Representative histograms are shown on the left, whereas data from multiple independent experiments are shown on the right. Numbers in histograms indicate MFI. (**B**) Expression of 2B4 on OT-I CD8$^+$ T cells from the indicated mice, activated or not with APCs plus antigen, was analyzed by flow cytometry. MFIs are shown. Isotype controls are depicted by the shaded histograms. Representative of three experiments. (**C**) Freshly isolated CD4$^+$ splenic T cells from WT, CD2 KO, or CD48 KO were activated with anti-CD3 (3 μg ml^{-1}) and anti-CD28 (1 μg ml^{-1}) and expanded in IL-2–containing medium. Fixed cells were then stained with fluorescently labeled anti-CD2 (red) and anti-CD48 (green) Abs. Cells were analyzed with a laser scanning confocal microscope. Representative photographs are shown on the left, whereas FI distribution along the dashed lines in the overlaid image is depicted on the right. Scale bars, 5 μm. (**D**) A FRET assay probing the proximity of CD2 and CD48 was performed by transfecting HEK293T cells with SNAP-tagged CD2 and CLIP-tagged CD48. CLIP-CD48 was then labeled with CLIP-Surface 547 (energy donor), whereas SNAP-CD2 was labeled with SNAP-Surface 647 (energy acceptor), followed by FRET analysis. Assays were performed in the presence or absence of blocking anti-CD2 RM2-5 or isotype control Ab. From left to right, images of pre- and postbleaching confocal microscopy analyses, calculated FRET efficiency images (the purple to yellow spectrum depicts weak to strong FRET), and dissolved inorganic carbon (DIC) images are shown. Statistics for FRET are on the complete right. $n = 12$ cells from three independent experiments. Scale bars, 5 μm. (**E** and **F**) Same as Fig. 1 (D and E), except that freshly isolated WT or CD48 KO OT-I splenic T cells stimulated with peptide-loaded splenocytes from WT or CD48 KO mice were analyzed. (**G**) Same as Fig. 1F, except that WT or CD48 KO OT-II T cells stimulated with peptide-loaded splenocytes from WT or CD48 KO mice were analyzed. Each symbol in (A) and (D) represents an individual mouse or cell; results in (E) to (G) are pooled from three independent experiments. One experiment representative of three independent experiments is shown in (B). Error bars represent means with SD. *$P \leq 0.05$, **$P \leq 0.01$, ***$P \leq 0.001$, ****$P \leq 0.0001$, ns $P > 0.05$ (two-sided unpaired Student's t tests).

T cell development or T cell subsets was observed in CD48 KO mice (fig. S2, B to E). As was the case for CD2 KO T cells (Fig. 1), CD48 KO T cells, either CD4+ or CD8+, displayed greatly reduced responses to anti-CD3 Abs, with or without anti-CD28 Abs, or to Con A ("C") when compared with WT T cells (fig. S3A). Analogous defects were observed upon stimulation with WT APCs and SEB or allogeneic WT BALB/c splenocytes (fig. S3, B and C). By opposition, when WT BALB/c CD8+ T cells were activated by CD48 KO splenic cells, no defect in alloreactivity was seen (fig. S3C). CD48 KO OT-I T cells and CD48 KO OT-II T cells also displayed markedly reduced responses to WT APCs and antigen compared with their WT OT-I or OT-II T cell counterparts, respectively (Fig. 2, E to G). These defects were seen whether APCs expressed CD48 or not. Once again, WT OT-I or OT-II T cells acti-vated by CD48 KO splenocytes as APCs plus antigen showed no defect.

Therefore, loss of CD48 on T cells mimicked the defects in T cell activation caused by loss of CD2, implying that the CD2-CD48 cis interactions were critical for T cell activation. Loss of CD48 on APCs had no appreciable impact on the responses studied.

CD48 on APCs is needed for CD2-dependent cytotoxicity

To examine whether CD2-CD48 cis interactions were needed for T cell–mediated cytotoxicity, OT-I CD8+ T cells from WT, CD2 KO, or CD48 KO mice were primed by a first stimulation with WT APCs and a high concentration of OVA peptide (Fig. 3A). After expansion in IL-2–containing medium, cytotoxicity was measured using EL-4 T cell lymphoma cell line, RMA T cell lymphoma cell line, or activated CD4+ T cells as target cells, loaded or not with the OVA peptide. All these targets normally express CD48. Using a 51Cr release assay, we found that WT T cells had marked cytotoxicity toward EL-4 cells in the presence of antigen but not in the absence of antigen (Fig. 3, B and C). This response was markedly com-promised in CD2 KO T cells (Fig. 3B). However, no defect was ob-served in CD48 KO T cells (Fig. 3C). Similar results were obtained when cell surface exposure of CD107a, a marker of degranulation, was assessed (fig. S4, A and B).

To assess whether CD2 was engaged by CD48 on target cells to promote cytotoxicity, similar experiments were conducted with RMA cells, either expressing CD48 or not, as targets (Fig. 3D). WT T cells displayed reduced cytotoxicity and diminished CD107a exposure in response to OVA peptide–loaded CD48− RMA compared with CD48+ RMA (Fig. 3, E and F, and fig. S4, C and D). In contrast, CD2 KO T cells had similar defects toward CD48+ and CD48− targets (Fig. 3E and fig. S4C). Although there was no difference in cytotoxicity mediated by WT or CD48 KO T cells toward CD48+ RMA, as shown above, CD48 KO T cells had more severe defects in cytotoxicity toward CD48− RMA compared with CD48+ RMA (Fig. 3F and fig. S4D). Similar results were obtained when CD4+ T cells were used as APCs (fig. S4, E and F). In contrast to cytotoxicity, proliferation and cytokine production by antigen-primed cytotoxic CD8+ T cells were not compromised by loss of CD48 on APCs (fig. S4G).

Thus, unlike proliferation and cytokine production, CD2-dependent cytotoxicity required expression of CD48 on APCs. When APCs lacked CD48, expression of CD48 on T cells enabled a partial com-pensation of cytotoxicity.

CD2 and CD48 expressed on T cells are critical for graft-versus-host disease

To validate these findings in vivo, we studied graft-versus-host disease (GVHD), a T cell–dependent immunopathology in which donor T cells

are activated by allogeneic MHC in the host, leading to T cell–dependent cytokine secretion and cytotoxicity toward host cells (19). Briefly, CD8+ T cells and CD4+ T cells (the latter to provide help) were purified from WT, CD2 KO, or CD48 KO mice in the B6 back-ground and injected in previously irradiated WT BALB/c mice (Fig. 4A). Weight loss and survival were monitored.

Whereas mice given phosphate-buffered saline (PBS) alone did not show weight loss or reduced survival, mice provided with WT T cells exhibited progressive weight loss (after ~day 5) and mortality (after ~day 9) (Fig. 4B). All mice given WT T cells died by day 16. In contrast, mice receiving CD2 KO T cells displayed less rapid weight loss and mortality. About 40% of these mice survived. Furthermore, after an initial weight loss, several mice gained back weight. Com-pared with mice injected with WT T cells, mice inoculated with CD48 KO T cells also had less severe weight loss and mortality. Nevertheless, this effect was not as pronounced as that seen in mice receiving CD2 KO T cells.

To examine whether the reduced GVHD in CD2 KO or CD48 KO mice was due to compromised T cell activation, mice were sac-rificed at day 7, before the onset of mortality (Fig. 4C). Donor T cells (identified by expression of H2-Kb) were enumerated in spleen and analyzed for expression of effector markers. Mice injected with PBS alone did not have donor T cells, as expected (Fig. 4, D and E). However, all other mice did. Mice injected with CD2 KO T or CD48 KO T cells had lower proportions and numbers (reduced by ~50 to 70%) of donor T cells compared with mice given WT T cells. This was true for CD8+ and CD4+ T cells. Nearly all donor T cells were CD44hiCD62Llo, indicating that they were activated (Fig. 4D).

To ensure that CD2 KO and CD48 KO T cells did not have a compromise in survival after transfer, we also sacrificed mice at day 3, before the onset of weight loss. Mice inoculated with WT, CD2 KO, or CD48 KO T cells displayed no difference in the proportions or numbers of donor T cells (Fig. 4F).

Therefore, the absence of CD2 or, to a lesser extent, CD48 on T cells resulted in reduced GVHD. This effect was not due to re-duced T cell survival but rather was due to compromised expansion of activated T cells. The intermediate defect observed with CD48 KO donor T cells, compared with CD2 KO T cells, was in keeping with a partial role of CD48 on APCs in cytotoxicity, which is in-volved in GVHD.

CD2 promotes T cell activation via proline-rich motifs in its cytoplasmic domain

Whereas CD48 is GPI-linked and lacks a cytoplasmic domain, CD2 is a transmembrane receptor bearing a cytoplasmic domain that has a conserved sequence across species (Fig. 5A). To determine whether CD2 mediates the signals promoting T cell activation during cis interactions, structure-function analyses of CD2 were performed. Mutants carrying proline-to-alanine substitutions in five conserved proline-rich motifs in the CD2 cytoplasmic segment, or a deletion of most of the CD2 cytoplasmic domain, were engineered (Fig. 5A). Then, constructs were retrovirally transduced in CD2 KO T cells. All mutants, in addition to WT CD2, rescued expression of CD2 on CD2 KO T cells (Fig. 5B). Upon stimulation with anti-CD3 Abs, CD2 KO T cells expressing WT CD2, but not green fluorescent pro-tein (GFP) alone, displayed a rescue of T cell activation responses, either proliferation or cytokine production (Fig. 5C). CD2 KO T cells expressing the CD2 variants having mutations in the first (P1), second (P2), or fifth (P5) proline-rich region were also rescued. In contrast,

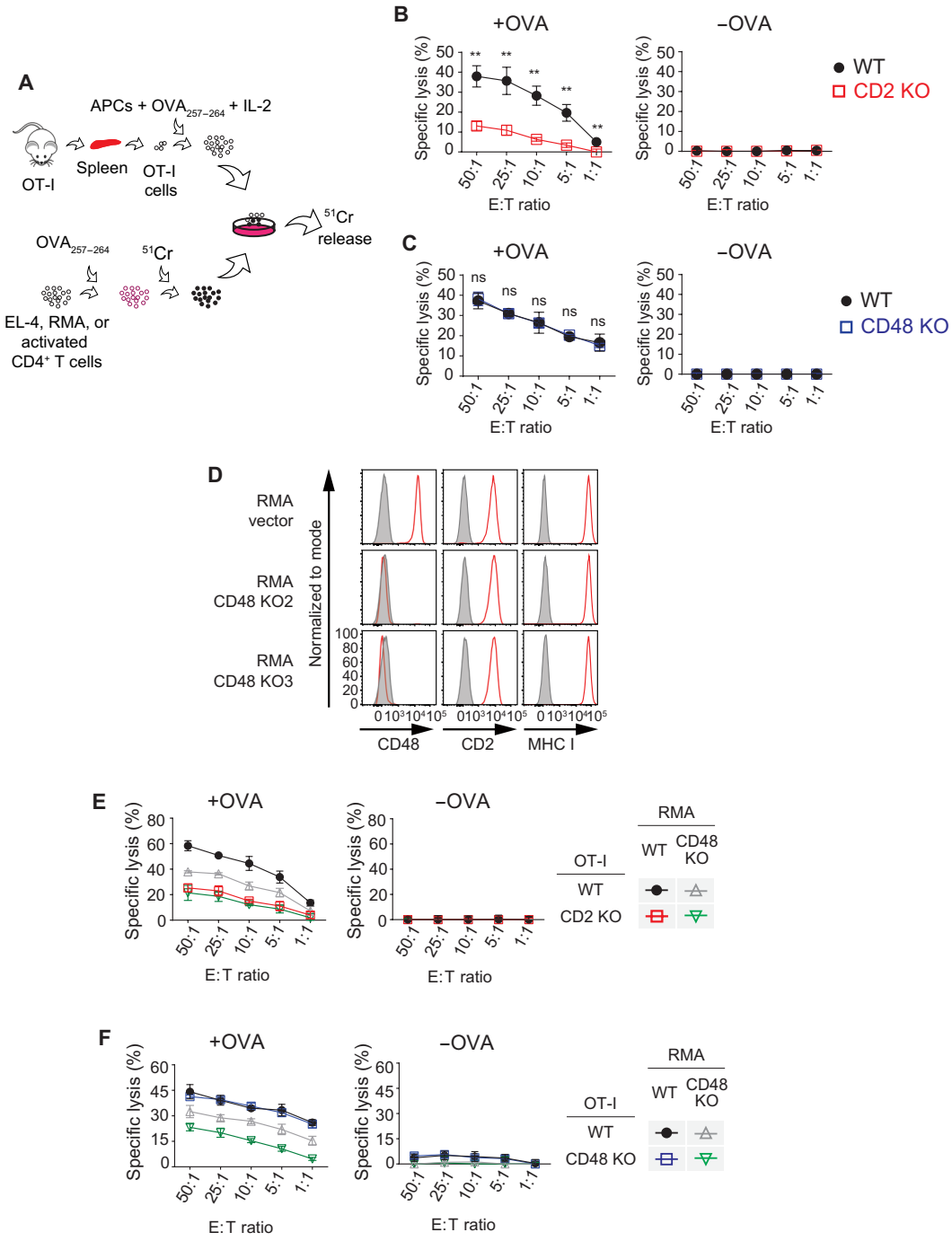

Fig. 3. CD48 on APCs is needed for CD2-dependent cytotoxicity. (**A**) Depiction of the protocol used for Fig. 3. Freshly isolated OT-I CD8$^+$ splenic T cells from WT, CD2 KO, or CD48 KO mice were primed with OVA peptide N4 (20 μM) + APCs and propagated in IL-2 (50 U ml^{-1}). Then, they were tested for cytotoxicity against EL-4, RMA, or activated CD4$^+$ T cells as targets, loaded or not with peptide. (**B**) Previously activated WT or CD2 KO OT-I CD8$^+$ T cells were stimulated with EL-4 in the presence or absence of OVA peptide N4 (1 μM) at the indicated E:T ratios. Cytotoxicity was determined using a chromium release assay. (**C**) Same as (B), except that previously activated WT or CD48 KO OT-I CD8$^+$ splenic T cells were analyzed. (**D**) Flow cytometry analyses showing expression of CD48, CD2, and MHC I (H-2K^b) on scrambled control or CD48 KO RMA cells (red lines). Two different targeting sequences were used to generate two different polyclonal CD48 KO derivatives. Isotype control is shown by shaded histograms. (**E**) As in (B), except that previously activated WT or CD2 KO OT-I CD8$^+$ splenic T cells were stimulated with RMA (expressing CD48 or not) in the presence or absence of OVA peptide (1 μM). (**F**) Same as (E), except that previously activated WT or CD48 KO OT-I CD8$^+$ splenic T cells were analyzed. Results are pooled from three independent experiments in (B), (C), (E), and (F). The results in (D) are representative of three independent experiments. Error bars represent means with SD. $^{**}P \leq 0.01$, ns $P > 0.05$ (two-sided unpaired Student's *t* tests).

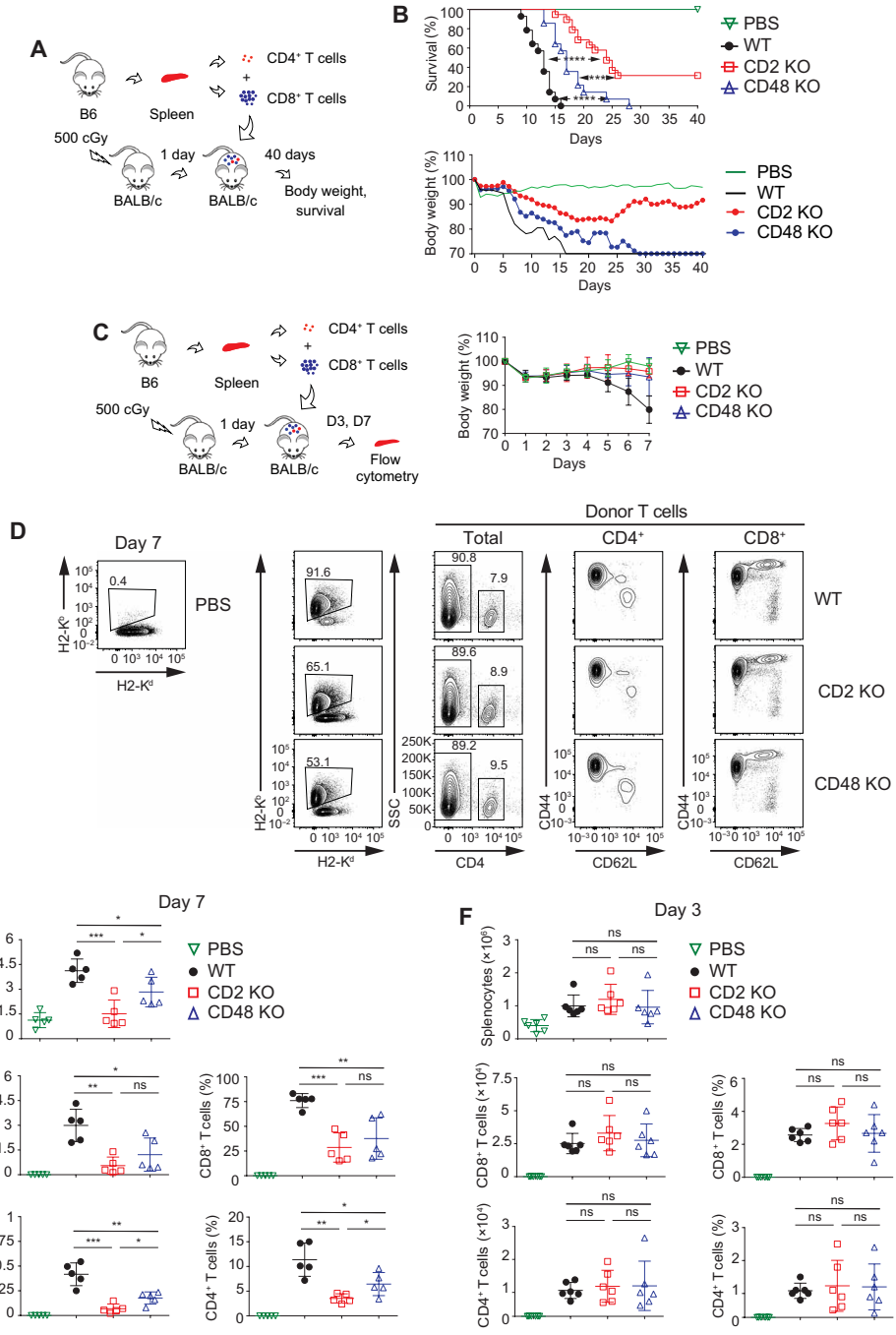

Fig. 4. CD2 and CD48 expressed on T cells are critical for GVHD. (**A**) Protocol of GVHD model. Freshly isolated $CD8^+$ splenic T cells and $CD4^+$ splenic T cells (3:1) from WT, CD2 KO, or CD48 KO mice (C57BL/6; B6) were injected in sublethally irradiated BALB/c mice (as recipient mice). Survival and body weight were monitored for 40 days. (**B**) Survival and body weight loss of BALB/c recipients after transplantation of donor T cells from WT, CD2 KO, or CD48 KO mice (B6). Control mice were injected with PBS alone. $n = 14$ (WT donor T cells), 19 (CD2 KO donor T cells), 14 (CD48 KO donor T cells), and 6 (PBS). The mean values of body weight of the surviving recipients are shown. (**C** to **F**) Same as (B), except that spleens of recipient mice were harvested on day 7 (D7) (D and E) or day 3 (D3) (F) after transplantation. (C) Protocol is depicted on the left, whereas body weight for the day 7 experiment is shown on the right. (D to F) Enumeration of donor T cells in spleens of recipient mice at day 7 (D and E) or day 3 (F) after transplantation. Splenocytes were stained with anti–class I MHC H-$2K^b$ (B6-specific), anti–class I MHC H-$2K^d$ (BALB/c-specific), anti-CD4, anti-CD62L, and anti-CD44. Donor $CD4^+$ T cells were identified as $CD4^+$H-$2K^{b+}$, whereas donor $CD8^+$ T cells were identified as $CD4^-$H-$2K^{b+}$. Representative flow cytometry analyses at day 7 are shown in (D). Specific populations with percentages are boxed. Data for cell numbers and percentages of multiple mice are represented in (E) and (F). $n = 5$ (WT donor T cells), 5 (CD2 KO donor T cells), 5 (CD48 KO donor T cells), and 5 (PBS) in (E). $n = 6$ (WT donor T cells), 6 (CD2 KO donor T cells), 6 (CD48 KO donor T cells), and 6 (PBS) in (F). Results are pooled from three independent experiments. Each symbol represents a mouse in (E) and (F). Error bars represent means with SD. For survival analyses, a log-rank (Mantel-Cox) test was performed. Otherwise, a two-tailed unpaired Student's *t* test was used. $^*P \le 0.05$, $^{**}P \le 0.01$, $^{***}P \le 0.001$, $^{****}P \le 0.0001$, ns $P > 0.05$ (two-sided unpaired Student's *t* tests).

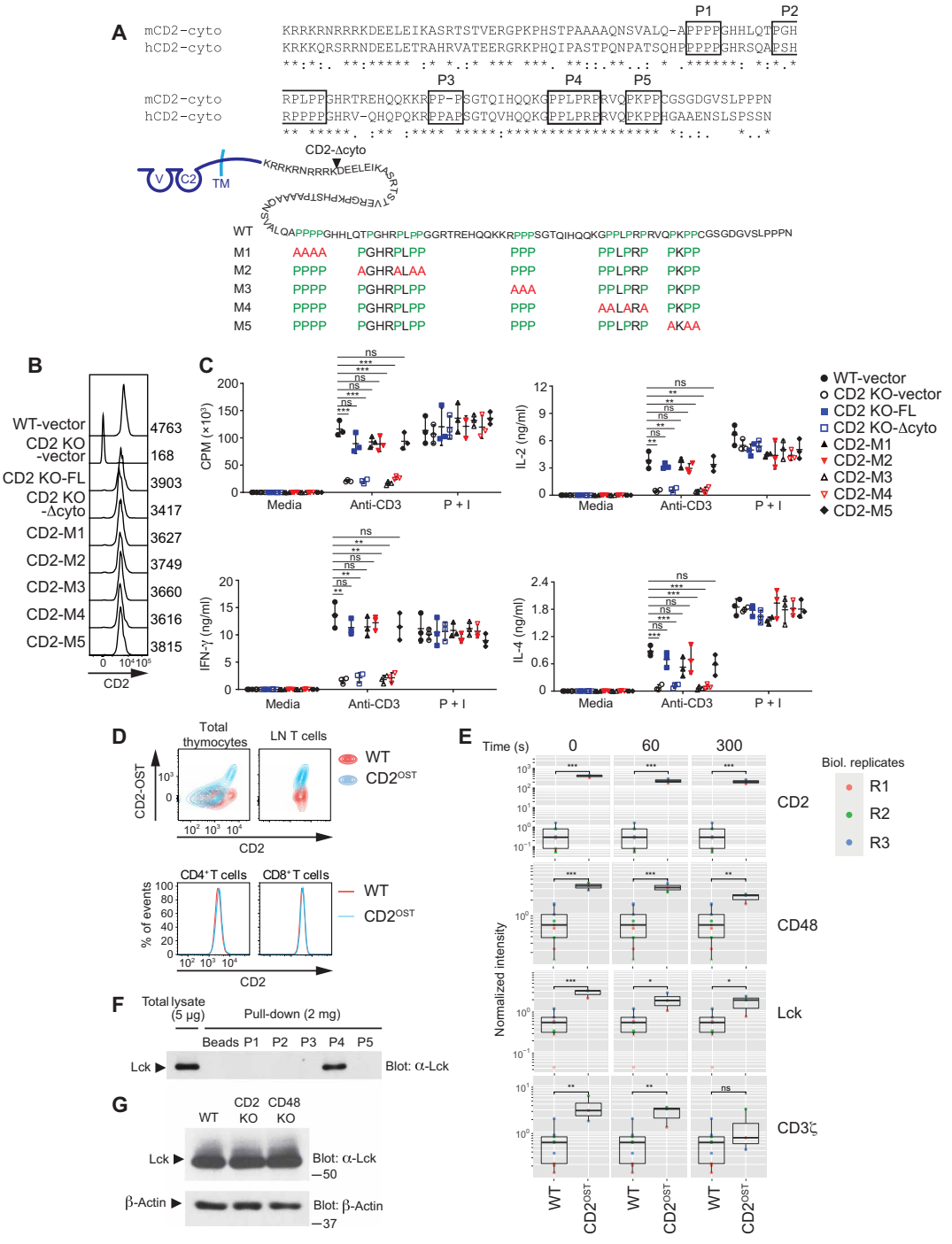

Fig. 5. Proline-rich regions in the CD2 cytoplasmic domain are necessary to promote T cell activation. (**A**) The sequences of the cytoplasmic domain of mouse and human CD2, in addition to the positions of the conserved proline-rich sequences, are shown at the top. Identical residues are marked with asterisks, whereas conserved residues with strongly similar properties are marked with colons and semiconserved residues with weakly similar properties are marked with periods. A schematic representation of the primary structure of CD2, the site of the truncation for the cytoplasmic domain–truncated mutant (Δcyto), and the locations of the five P-to-A mutants (M1 to M5) is found at the bottom. P1, P2, P3, P4, and P5 depict the five proline-rich regions from CD2 cytoplasmic domain. TM, transmembrane domain; V, Ig-like V-type domain; C2, Ig-like C2-type domain. (**B** and **C**) Previously activated CD4$^+$ splenic T cells from the indicated mice were infected with retroviruses encoding GFP alone or in combination with full-length or mutated CD2. (B) After sorting of GFP-positive cells, expression of CD2 was verified by flow cytometry. FL, full-length. MFIs are shown on the right. Representative of $n = 3$. (C) Sorted cells were stimulated with anti-CD3 alone or P + I. Activation was monitored as Fig. 1A. (**D**) Total thymocytes and lymph node (LN) T cells (gated on TCR$^+$ cells) isolated from mice with the specified genotypes were permeabilized and stained with Strep-Tactin APC plus anti-CD2 and analyzed by flow cytometry (top). Expression of CD2 in CD4$^+$ and CD8$^+$ T cells from LN of WT and CD2^{OST} mice (bottom). (**E**) The abundances of the CD2 interactors specified on the right were estimated for each time point and biological replicate (R1, R2, and R3). Normalized intensities (see Materials and Methods) for WT and CD2^{OST} cells were compared using a two-sided Welch *t* test. Imputed missing values are represented with lighter shaded dots. (**F**) Pull-down assay. Biotinylated peptides encompassing each of the five proline-rich sequences of CD2 were synthesized and coupled to avidin beads. They were then incubated with previously activated CD4$^+$ splenic T cell lysates. After several washes, the presence of Lck was detected by immunoblotting. Representative of $n = 3$. (**G**) Expression of Lck in purified splenic CD4$^+$ T cells was analyzed by anti-Lck immunoblotting (top). Expression of β-actin was used as loading control (bottom). Representative of $n = 3$. Results are pooled from three independent experiments in (C). Each symbol represents a mouse. Error bars represent means with SD. *$P \leq 0.05$, **$P \leq 0.01$, ***$P \leq 0.001$, ****$P \leq 0.0001$, ns $P > 0.05$ (two-sided unpaired Student's *t* tests, unless specified otherwise).

though, cells that contained the CD2 mutants lacking the cytoplas-mic domain, or having mutations in the third (P3) or fourth (P4) proline-rich region, were not rescued. Hence, the cytoplasmic do-main of CD2, in particular two of its proline-rich motifs, was criti-cal for the ability of CD2 to promote T cell activation.

Ability of CD2 to promote T cell activation correlates with binding to kinase Lck

To elucidate further the mechanism of CD2 signaling, we generated a gene-targeted knock-in mouse in which the CD2 protein was tagged at its C terminus with a One-STrEP-tag (OST) tag, which enables affinity purification (AP) with streptavidin (20, 21). Heterozygous knock-in mice were used for our studies. Compared with those of WT mice, T cells from CD2OST mice displayed normal development and expression of CD2, with the exception that the variant CD2, but not endogenous CD2, was recognized by anti-OST Abs (Fig. 5D).

Then, previously activated CD4+ T cells from CD2OST mice were left unstimulated or stimulated for 1 or 5 min with anti-CD2 Abs in an attempt to enhance engagement of CD2. After lysing cells in maltoside-containing buffer, OST-tagged CD2 was recovered with Strep-Tactin Sepharose beads, and associated proteins were detected and quantified by mass spectrometry (MS). We identified 68 high-confidence CD2-interacting proteins that showed a greater than threefold enrichment, with a P value below 0.05 in at least two of the three conditions of stimulation (table S1). As expected, the CD2-CD48 interaction ($P = 0.00015$, in unstimulated cells) was detected regardless of the stimulation condition. No other GPI-linked pro-tein was detected using these stringency criteria. However, when the enrichment fold was reduced to 2, GPI-linked Thy-1 was also noted, although the statistical significance was lower ($P = 0.017$) and was significant only in unstimulated cells (table S1). Among the high-confidence interactors, we also identified the kinase protein tyrosine kinase Lck, as well as the CD3z and CD3g chains of the TCR com-plex (Fig. 5E and table S1). As with CD48, these interactions were seen whether cells were treated or not with anti-CD2 Abs. Previously described CD2-interacting proteins such as Fyn, Itk, CD2AP, and CD2BP1 were not observed.

To examine whether one or more of the proline-rich motifs of CD2 might recruit Lck, which bears an Src homology 3 domain capable of binding proline-rich motifs, pull-down assays were per-formed. Biotinylated peptides corresponding to each of the five proline-rich sequences of CD2 were synthesized and coupled to avi-din beads. They were incubated with T cell lysates, and the presence of Lck was detected by immunoblotting. The peptide encompassing the fourth proline-rich region (P4), but not the other peptides or beads alone, was able to recover Lck (Fig. 5F). No difference in expression of Lck was noted between WT, CD2 KO, and CD48 KO T cells (Fig. 5G).

Therefore, CD2 interacted with several proteins, including Lck and components of the TCR complex. These interactions were ob-served in unstimulated cells, in keeping with the idea that CD2 and CD48 were interacting before TCR stimulation. We also found that one of the proline-rich regions of CD2 necessary to promote T cell activation, P4, bound to Lck in vitro.

Cis interactions between CD2 and CD48 are required for TCR signaling

Engagement of the TCR triggers multiple signals initiated by the protein tyrosine kinases Lck, Fyn, and ZAP-70 (1–3). To determine how CD2-CD48 cis interactions enabled proper T cell activation, TCR-mediated signals were analyzed. Engagement of the TCR by anti-TCR Abs on CD2 KO or CD48 KO T cells resulted in compro-mised protein tyrosine phosphorylation compared with WT T cells (Fig. 6A). This change mostly affected substrates of 36, 76, and 120 kDa. There was also a reduction in TCR-evoked activation of the kinase extracellular signal–regulated kinase (Erk) and calcium fluxes, two proximal responses downstream of protein tyrosine phosphorylation, and in TCR-triggered expression of CD25,

a more distal feature of T cell activation (Fig. 6, B to D). Similar calcium flux and CD25 expression defects were seen with Con A. For all signals, the impacts of CD2 or CD48 deficiency were equivalent (Fig. 6, A to D).

Last, to ascertain whether interactions between CD2 and CD48 expressed on adjacent T cells (cisT-T interactions) could rescue the defects in TCR signaling seen in CD2 KO or CD48 KO T cells, these two cell populations were mixed 1:1 before cell activation. To dis-tinguish the two cell populations, CD2 KO mice were first bred with B6.SJL mice, which express CD45.1 instead of CD45.2. Expression of CD45.1 was used to distinguish CD2 KO (CD45.1+) and CD48 KO (CD45.1−) T cells (Fig. 6E). When CD2 KO T cells and CD48 KO T cells were mixed, there was no correction of the defect in cal-cium fluxes triggered by anti-TCR Ab or Con A in either cell type (Fig. 6E).

Thus, the CD2-CD48 cis interactions were required for proximal TCR signals. This effect required coexpression of CD2 and CD48 on the same cell.

Cis interactions of CD2 and CD58 promote human T cell activation

In humans, CD2 interacts with CD58, which, like mouse CD48, is GPI-linked and expressed not only on APCs but also on T cells (6, 8). Although human CD2 can interact with human CD48, this inter-action was described to be of much lower affinity (22). To ascertain whether a function analogous to that of CD2-CD48 in mouse T cells was provided by CD2-CD58 in human T cells, the impact of loss of CD2 or CD58 (or CD48, as control) was evaluated, using the human T cell line Jurkat, which normally expresses CD2, CD58, and CD48. Variants of Jurkat lacking CD2, CD58, or CD48 were generated by CRISPR-Cas, using two different guide RNAs for each molecule (fig. S5A).

In binding assays using soluble Fc fusion proteins, CD2 KO cells failed to bind CD58-Fc, whereas CD58 KO cells did not react with CD2-Fc, when compared with control Jurkat cells (Fig. 7A and fig. S5B). In addition, as was the case for mouse cells, CD2 KO cells had augmented (~10-fold) binding to CD2-Fc, whereas CD58 KO cells showed increased (~3-fold) staining with CD58-Fc. Cells minimally bound to CD48-Fc, with the exception of CD48 KO cells, which displayed augmented staining.

From a functional point of view, CD2 KO and CD58 KO cells, but not CD48 KO cells, displayed markedly reduced protein tyro-sine phosphorylation and calcium fluxes in response to anti-TCR Abs or the lectin phytohemagglutinin (PHA) (Fig. 7, B and C). In addition, CD2 KO and CD58 KO cells, but not CD48 KO cells, had a pronounced decrease in anti-CD3 Ab–induced production of IL-2 compared with control cells (Fig. 7D). No difference was seen with PMA plus ionomycin. Hence, CD2 and CD58 formed an exclusive receptor-ligand pair in human T cells. Coexpression of CD2 and CD58, but not of CD48, was critical for TCR signaling and T cell activation.

DISCUSSION

By creating new KO mouse strains in a pure B6 genetic background and using blocking anti-CD2 Abs, we found that CD2 was critical for T cell activation in response to a variety of stimuli, including antigen, superantigen, alloantigen, mitogenic lectins, and anti–TCR- CD3 Abs without or with anti-CD28 Abs. In contrast, CD2 was not needed for activation by PMA plus ionomycin. An identical role was ascribed to T cell–expressed CD48, the sole ligand of CD2 in mice. Because the activation defects observed in CD2 KO or CD48 KO T cells occurred in cells stimulated with anti-TCR Abs without

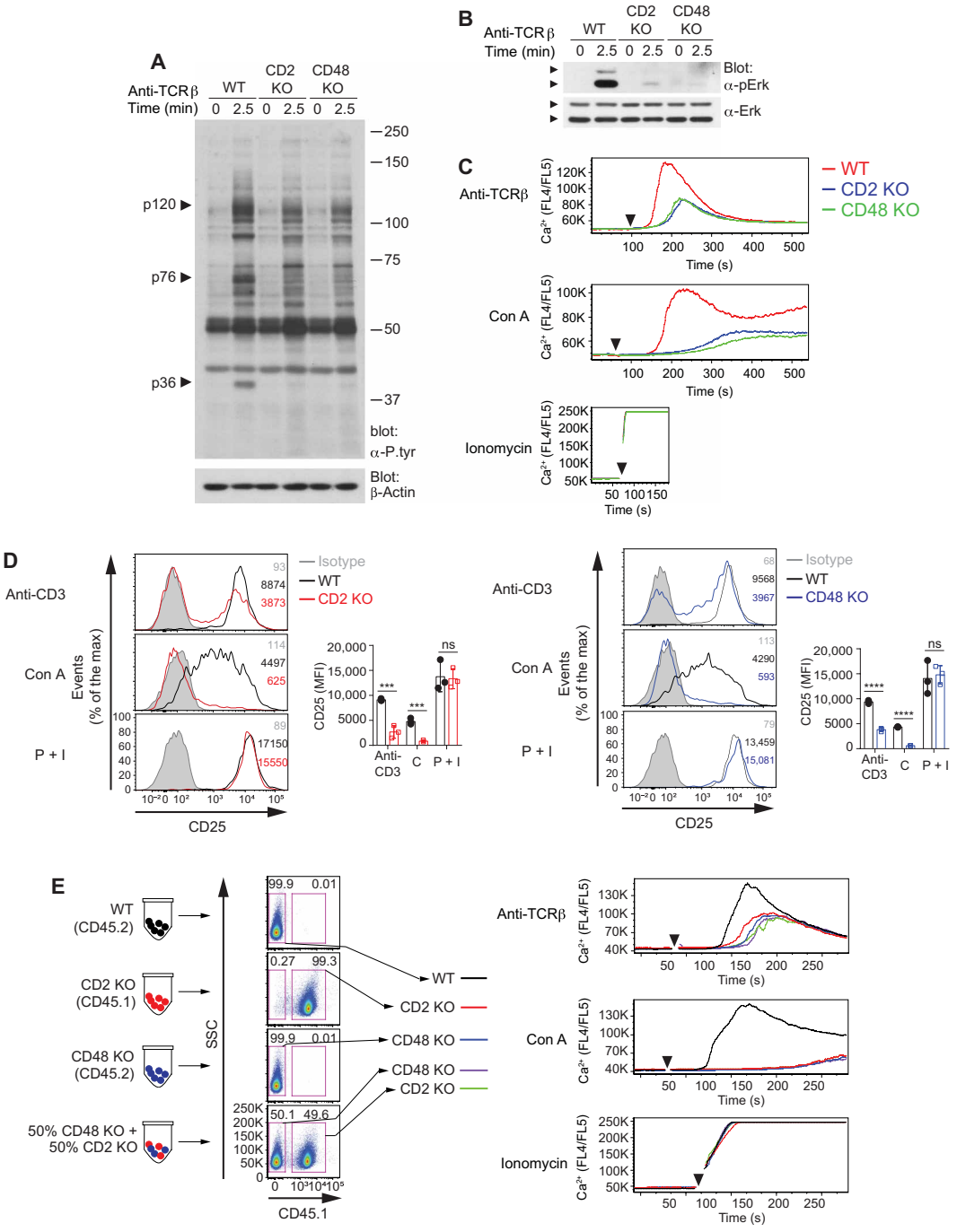

Fig. 6. Cis interactions between CD2 and CD48 are required for maximal TCR signaling. (**A** and **B**) Freshly isolated splenic CD4$^+$ T cells from the indicated mice were incubated for 0 and 2.5 min with biotinylated anti-TCRβ (5 μg ml^{-1}), followed by avidin (10 μg ml^{-1}). Phosphotyrosine (P.tyr)–containing proteins were detected by immunoblotting of total cell lysates with anti (α)–P.tyr (A), whereas activation of Erk was monitored by immunoblotting with phospho-specific Abs recognizing activated Erk (pErk) (B). β-actin and total Erk were studied in parallel as loading controls. The positions of molecular mass markers are shown on the right. (**C**) Freshly isolated splenic CD4$^+$ T cells were loaded with Indo-1 and stimulated with anti-TCRβ (0.5 μg ml^{-1}), Con A (4 μg ml^{-1}), or ionomycin (1 μg ml^{-1}). Changes in intracellular calcium were determined by ascertaining the fluorescence UV450/UV530 ratio (FL4/FL5), with a BD LSR flow cytometer. Arrowheads indicate when the stimulus was added. (**D**) Freshly isolated splenic CD4$^+$ T cells from the indicated mice were stimulated for 48 hours with anti-CD3 (3 μg ml^{-1}), Con A (4 μg ml^{-1}), or PMA (100 ng ml^{-1}) plus ionomycin (1 μg ml^{-1}) (P + I). Flow cytometry analyses of CD25 expression are shown. Isotype-matched rat IgG1 was used as control. A representative experiment is shown on the left, whereas data from multiple mice are summarized on the right. Numbers in histograms indicate MFI. (**E**) The indicated cells were mixed or not at a 1:1 ratio. Calcium fluxes triggered by anti-TCRβ Ab, Con A, or ionomycin were then studied. Protocol is depicted on the left, whereas changes in intracellular calcium are shown on the right. Staining for CD45.1 was used to distinguish CD2 KO cells (CD45.1$^+$) from the other cells (CD45.1$^-$). Representatives of three experiments are shown in (A) to (C) and (E). Each symbol represents a mouse in (D). Error bars represent means with SD. ***$P \leq 0.001$, ****$P \leq 0.0001$, ns $P > 0.05$ (two-sided unpaired Student's t tests, unless specified otherwise).

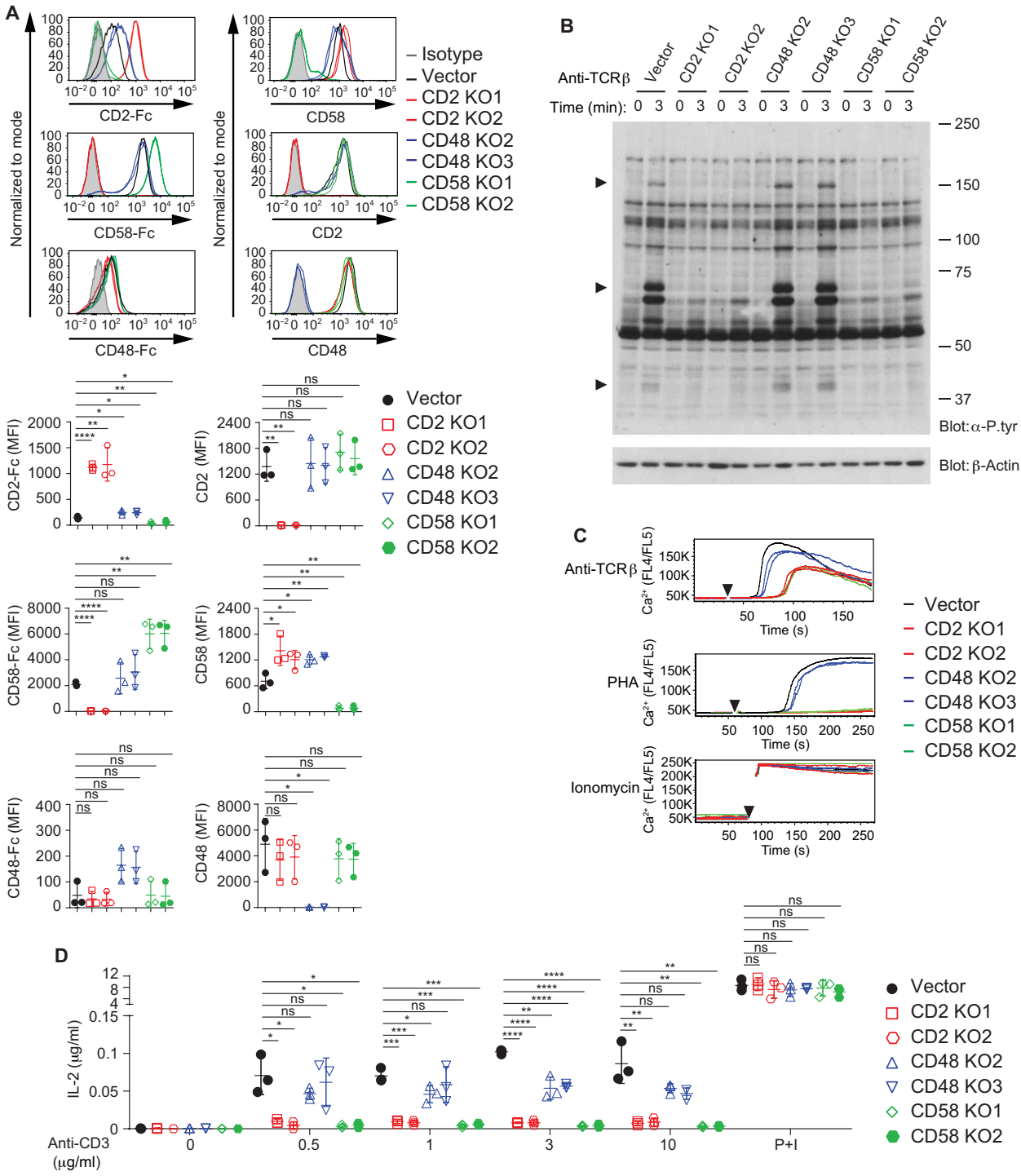

Fig. 7. Cis interactions of CD2 and CD58 promote human T cell activation. Polyclonal populations of Jurkat cells lacking CD2, CD58, or CD48 were generated by CRISPR-Cas9–mediated genome editing, using two different guide RNAs for each of these molecules. Jurkat cells transfected with empty vector alone were used as control. (**A**) Cells were stained with Fc fusion proteins encompassing the extracellular domain of CD2, CD58, or CD48, followed by a secondary Ab directed against the Fc segment of the fusion proteins. Expression of CD2, CD58, and CD48 was analyzed in parallel by staining cells with Abs directed against these molecules (red lines). Shaded histograms, isotype control. Representative histograms are shown at the top, whereas data from multiple independent experiments are shown at the bottom. Each symbol represents an individual experiment. (**B**) Same as Fig. 6A, except that variants of Jurkat cells were analyzed. A representative of three experiments is shown. (**C**) Same as Fig. 6C, except that variants of Jurkat cells stimulated with anti-TCRβ (top, 1 μg ml^{-1}), the lectin PHA (middle, 10 μg ml^{-1}), or ionomycin (bottom, 1 μg ml^{-1}) were studied. A representative of three experiments is shown. (**D**) Variants of Jurkat cells were stimulated with the indicated concentrations of anti-CD3 mAb OKT3 or PMA (100 ng ml^{-1}) plus ionomycin (1 μg ml^{-1}) (P + I). After 48 hours, production of IL-2 was determined by ELISA. Results are pooled from three independent experiments. Each symbol represents an individual experiment; error bars represent means with SD. *$P \leq 0.05$, **$P \leq 0.01$, ***$P \leq 0.001$, ****$P \leq 0.0001$, ns $P > 0.05$ (two-sided unpaired Student's *t* tests).

APCs, these data implied that CD2 and CD48 were interacting with each other on T cells and that these interactions were needed for T cell activation.

Our data indicated that the interactions between CD2 and CD48 on T cells occurred within individual T cells (cisT interactions). In support of this idea, we found that CD2 and CD48 were colocalized at the surface of individual T cells in immunofluorescence assays combined with confocal microscopy. Moreover, CD2 and CD48 were colocalized at the surface of transfected HEK293T cells in FRET as-says. The latter proximity was compromised by addition of a block-ing anti-CD2 Ab, which was also found to prevent activation when provided to WT T cells. Last, experiments in which CD2 KO T cells and CD48 T cells were mixed indicated that the presence of adja-cent cells expressing the missing component of the receptor-ligand pair could not rescue TCR-triggered calcium fluxes in mutant T cells. As suggested for cis interactions involving other molecules (23), we postulate that the CD2-CD48 cis interactions occurred head to head. It is possible that both molecules positioned themselves to lay flat on the plasma membrane, as suggested for class I MHC (24), there-by enabling interaction with each other. Alternatively, it is possible that the interactions were facilitated by membrane curvatures or mem-brane microvilli, which exist in T cells (fig. S5C). They may be facil-itated by the formation of microdomains centered around CD2 and other signaling molecules, as suggested by Douglass and Vale (25).

Although our results provided solid evidence that CD2-CD48 cis interactions took place in individual T cells, it should be pointed out that they did not exclude the possibility that CD2 and CD48 may also interact between adjacent T cells (cisT-T interactions) under certain conditions. This may be especially prominent when T cells are juxtaposed, for instance, as a consequence of T cell adhesion to APCs or as a result of T cell homotypic clustering during T cell pro-liferation. These possibilities deserve future consideration.

When T cells were activated by antigens and APCs, the presence of CD48 on APCs was not needed for proliferation and cytokine production. This was true in freshly isolated T cells and previously activated T cells. However, expression of CD48 on APCs, as well as on T cells, was needed for CD8+ T cell–mediated cytotoxicity. This dual involvement of CD48 was in keeping with our observation that GVHD, a T cell–dependent model of immunopathology involving cytotoxicity, was more compromised in CD2 KO mice compared with CD48 KO mice. We postulate that CD2-CD48 interactions in trans are also required for cytotoxicity because of the need of trans interactions to facilitate the release of cytotoxic granules toward tar-get cells. Evidence of a key role of engagement of CD2 on human T cells by CD58 on APCs was provided by others for polarization of cytotoxic granules toward the microtubule-organizing center (10).

Structure-function analyses of CD2 indicated that the cytoplas-mic domain of CD2 was essential for its capacity to enhance T cell activation. Moreover, mutation of either of two proline-rich motifs, M3 and M4, abolished the activating function. One of these proline- rich regions, M4, was able to bind to Lck in vitro. Coupled with the observations that CD2 coimmunoprecipitated with components of the TCR complex in the CD2OST mouse and that CD2-CD48 cis interactions increased TCR-elicited protein tyrosine phosphoryl-ation, these data suggested that CD2 enhanced T cell activation by recruiting Lck in the vicinity of the TCR complex (fig. S5C).

Further support for this idea was provided by our biochemical studies showing that CD2 and CD48 augmented TCR-triggered protein tyrosine phosphorylation, the most proximal TCR-induced signal. This effect was not global but rather selectively affected tyro-sine phosphorylation substrates of 36, 76, and 120 kDa, which possibly represented LAT, SLP-76, and c-Cbl. CD2-CD48 also augmented TCR-elicited calcium fluxes and Erk activation, two downstream effectors of phospholipase C (PLC)–g1,

which is activated in response to TCR stimulation. Although proximal TCR signaling was enhanced by CD2-CD48 cis interactions, it is unclear why TCR-evoked pro-tein tyrosine phosphorylation was not globally augmented. Perhaps only part of the TCR signalosome was influenced by CD2-CD48.

On the basis of our MS data using previously activated T cells from CD2OST mice, the interactions of CD2, CD48, and TCR seemed to be constitutive and to precede engagement of TCR by ligands. Whether this is only a feature of previously activated T cells or whether this is also seen with naïve T cells remains to be clarified. In any case, we presume that active CD2 signaling in the absence of TCR engagement was prevented because of the high activity of pro-tein tyrosine phosphatases, in particular CD45, in the vicinity of TCR. TCR engagement is known to sequester the TCR complex from CD45 to facilitate TCR signaling (26).

Previous studies had provided evidence for a mitigated role of CD2 and CD48 in T cell activation that was primarily limited to low- affinity antigens or low concentrations of anti-CD3 Abs. However, our data showed that CD2 and CD48 have a broad key role in normal T cell activation, including in response to high-affinity antigens. Perhaps the differences between the previous results and ours related to the fact that, in the earlier studies, mice in a mixed 129/B6 background were used. A mixed 129/B6 background is notoriously problematic for studies involving SLAM family receptors (27).

Although CD48 also exists in humans, it is not the primary ligand of CD2. The dominant ligand of CD2 in humans is CD58 (6, 22). We confirmed these findings herein. Using Jurkat as a human T cell model, we observed that CD2 and CD58 in Jurkat enhanced TCR-evoked signals and T cell activation, leading to cytokine production. CD48 had no impact on these responses. Hence, like CD2 and CD48 in mice, CD2 and CD58 in humans interact in cis at the sur-face of T cells to promote TCR signaling and T cell activation. Even if the identity of the CD2 ligands is not conserved across species, the importance of cis interactions for the function of CD2 is preserved. Given that CD58 is more highly expressed in human effector-memory and innate-like T cells compared with naïve T cells, the role of the CD2-CD58 cis interactions may be especially prominent in the for-mer cell types.

In published models, receptor-ligand interactions are typically depicted as occurring in trans. However, many receptors and their ligands are coexpressed on the same cell, raising the possibility that cis interactions can also take place. Firm evidence for the existence of cis interactions within individual cells has been provided for sev-eral receptor-ligand pairs in immune cells. Examples include PD-1 and its ligand PD-L1, which are coexpressed on APCs (23). In this case, the cis interactions interfere with the trans interactions, thereby suppressing the function of PD-1. Likewise, inhibitory Ly49 recep-tors and class I MHC can interact in cis on NK cells, thus attenuating the function of Ly49 in NK cells (28). Last, CD8 was shown to inter-act in cis with class I MHC at the surface of T cells, thereby compro-mising the function of CD8 in T cells (29).

In all these cases, the trans interactions were believed to pre-dominate functionally over the cis interactions. Moreover, the cis interactions were found to suppress the impact of the trans inter-actions. However, these features do not apply to the cis interactions between CD2 and its ligands in T cells. Our data suggested that the CD2-CD48 cis interactions functionally predominated over the trans CD2-CD48 interactions for most T cell activation responses. In addi-tion, either cis or trans CD2-CD48 interactions promoted T cell activation, and, in the case of cytotoxicity, these effects were syner-gistic. Whether these distinctive characteristics of the CD2-mediated cis interactions apply to cis interactions involving other molecules should be assessed. As a corollary, the possibility of targeting cis interactions to alter the functions of immune cell receptors for thera-peutic purposes deserves greater consideration.

MATERIALS AND METHODS

Study design

To address the role and importance of CD2 and its interactions with ligands (CD48 in mice and CD58 in humans) in T cells, new strains of KO mice lacking CD2 or CD48 were created in the C57BL/6 background. Analyses of T cell development and T cell activation responses, using T cells from these mice and APCs lacking CD48 or not were performed. Studies of mouse GVHD, a model of T cell autoreactivity, were conducted. Biochemical studies, structure- function analyses, and imaging approaches were used to ascertain the molecular mechanisms by which CD2 and CD48 promote T cell activation. Similar studies were performed for human CD2 and CD58, with the human T cell line Jurkat. For the studies using mice, animals with the proper genotype were randomly chosen, following the criteria outlined here. Numbers of mice and of experimental replicates were defined on the basis of established standards in the field and previous experience. No mice were excluded. Studies were not blinded.

Mice

CD2 KO mice and CD48 KO mice were generated by CRISPR- Cas9–based genome editing, using the plasmid pSpCas9(BB) (formerly pX330; Addgene) and the guide RNA sequences 5′-TGA-TATTGATGAGGTGCGAT-3′ (for CD2) and 5′-GGTTA-CATTGCTGCCGGTGG-3′ (for CD48). DNA was injected in fertilized oocytes of C57BL/6J mice (the Jackson Laboratory, Bar Harbor, ME). Mice were then screened by polymerase chain reac-tion (PCR) and by sequencing of the CD2-encoding (Cd2) or CD48-encoding (Slamf2) genes. For CD2 KO mice, mice bearing a 28-nucleotide (clone 914) or 25-nucleotide (clone 919) deletion in exon 2 of Cd2 were identified. For CD48 KO mice, mice bearing a 10-nucleotide (clone T6), a 1-nucleotide (clone T87), or a 147- nucleotide (clone del-147) deletion in exon 2 of Slamf2 were selected. Once identified, heterozygous KO mice were backcrossed to the C57BL/6J background for 10 to 12 (CD2 KO) or 6 to 12 (CD48 KO) generations and subsequently bred to homozygosity for experimentation. All deletions resulted in a frameshift in the second coding exon of the Cd2 or Slamf2 gene and caused loss of CD2 or CD48 expression by flow cytometry. For the generation of the CD2OST (C57BL/6NRj-Cd2tm1Ciphe) mouse, the mouse Cd2 gene was edited using a double-stranded homology-directed repair (HDR) template (targeting vector) with 1000-bp-long 5′ and 3′ homology arms. It included a Twin-Strep-tag–coding sequence (OST) inserted at the end of the last exon (exon 5) of the Cd2 gene and a self-excising tACE–Cre/Neor (ACN) cassette that was introduced at the beginning of the 3′ untranslated region sequence. The final targeting vector was abutted to a cassette coding for the diphtheria toxin fragment A (30–32).

The protospacer adjacent motif present in the targeting vector was destroyed via a silent mutation to prevent CRISPR-Cas9 cleavage. Two single-guide RNA (sgRNA)–specifying oligonucleotide sequences (5′-CTGCCGCCCCCTAATTAAGA-3′ and 5′-CCTAATTAAGAAG-GCAGAGT-3′) were annealed, generating overhangs for ligation into the Bbs I site of plasmid pX330 (pSpCas9; Addgene, plasmid ID 42230). JM8.F6 C57BL/6N embryonic stem (ES) cells (33) were electroporated with 20 mg of targeting vector and 2.5 mg of sgRNA-containing pX330 plasmid. After selection in G418, ES cell clones were screened for proper homologous recombination by Southern blot or PCR analysis. A neomycin-specific probe was used to ensure that adven-titious nonhomologous recombination events had not occurred in the selected ES clones. After blastocyst injection of mutant ES cells and germline transmission, screening for proper deletion of the ACN cassette and for the presence of the sequence coding for the OST was performed by PCR using the following pair of primers: sense 5′-CAGATTCACCAGCAGAAAG-3′ and antisense 5′-TGGGT C-CTACTTCCATTAAA-3′. This pair of primers amplified a 391-bp band and a 204-bp band in the case of the Cd2OST allele and the WT Cd2 allele, respectively. OT-I TCR transgenic mice

[C57BL/6-Tg(TcraTcrb) 1100Mjb/J] and OT-II TCR transgenic mice [B6.Cg-Tg(TcraTcrb) 425Cbn/J] were obtained from the Jackson Laboratory and bred with CD2 KO or CD48 KO mice. B6.SJL (B6.SJL-Ptprca Pepcb/BoyJ) mice were purchased from the Jackson Laboratory and bred with CD2 KO mice. BALB/c mice (BALB/cJ) were purchased from the Jackson Laboratory.

All mice were maintained in the C57BL/6J background unless specified. All animals were kept in a specific pathogen–free environ-ment. Sex- and age-matched mice between 7 and 12 weeks of age were used for experiments. Littermates were used whenever possible, except for the reactivation studies comparing CD2 KO OT-I mice and CD48 KO OT-I mice. Animal experimentation at Institut de recherches cliniques de Montréal was approved by the Animal Care Committee of the Institut de recherches cliniques de Montréal and performed as defined by the Canadian Council of Animal Care. Mice maintained at the Centre d'immunophénomique were handled in accordance with national and European laws for laboratory animal welfare and experimentation (EEC Council Directive 2010/63/EU, September 2010), and protocols were approved by the Marseille Ethical Committee for Animal Experimentation. No animals were excluded from the analyses.

Cells and retroviral infection

Thymocytes or splenocytes were harvested from the indicated mice. Red blood cells (RBCs) were depleted with RBC lysis buffer (Sigma- Aldrich, R7757) at room temperature for 5 min. CD4+ or CD8+ T cells, depleted of NK T cells using anti-NK1.1 monoclonal Abs (mAbs), were purified by negative selection from spleen using the EasySep Purification Kits (STEMCELL Technologies Inc., 19852 and 19853). Cell purity was consistently greater than 90%. EL-4 and RMA (T cell lymphoma), and RMA lacking CD48, were described (34–36). Jurkat (clone E6-1; T lymphoblast) was obtained from the American Type Culture Collection (Manassas, VA, USA). Jurkat T cells deficient of CD2, CD48, or CD58 were generated by the CRISPR- Cas9 system using the plasmid pSpCas9(BB)-2A-GFP (Addgene, plasmid #48138) and the guide RNA sequences 5′-CACCGAAGCT-GGCTACAAATTTACA-3′ and 5′-CACCGCTTGGGTCAGG-ACATCAACT-3′ (for CD2), 5′-CACCGTCACTTGGTACATA TGACCG-3′ and 5′-CACCGCTGGTCGAAAGTATAAAACC-3′ (for CD48), and 5′-CACCGTGGTTGCTGGGAGCGACGCG-3′ and 5′-CACCGAGACCACGCTGAGGACCCCC-3′ (for CD58). Plasmids were transfected into Jurkat cells by electroporation (Gene Pulser Xcell, Bio-Rad). Cells having lost the expression of targeted genes were sorted using the BD FACSAria III Cell Sorter (BD Bio-sciences). Lack of expression was confirmed by flow cytometry. Constructs encoding WT, cytoplasmic domain–deleted (Dcyto), or proline (P)–to–alanine (A) mutated (M1: P276A, P277A, P278A, and P279A; M2: P286A, P290A, P292A, and P293A; M3: P306A, P307A, and P308A; M4: P319A, P320A, P322A, and P324A; M5: P328A, P330A, and P331A) versions of mouse CD2 were generated by PCR and cloned into the pMSCV-MIGR-GFP retroviral vector, which also encodes GFP. Previously activated mouse CD4+ T cells were infected as described elsewhere (18, 37). Briefly, activated CD4+ T cells were obtained by stimulating purified CD4+ T cells with anti-CD3 (3 mg ml−1) plus anti-CD28 (1 mg ml−1) mAbs in the presence of mouse IL-2 (50 U ml−1). Infectious retroviral particles were recovered from the supernatant of Phoenix-Eco packaging cells transfected with the indicated retroviral constructs. Freshly harvested supernatants were added to the T cells, and cells were infected by spinfection (1000g for 60 min at 32°C). Cells infected with empty vector retroviruses were used as control. At day 4 after infection, GFP- positive cells were sorted (BD FACSAria III cell sorter, BD Biosciences), expanded in IL-2 (50 U ml−1), and then used for experimentation.

Plasmids

For production of the Fc fusion proteins encompassing the extra-cellular domain of mouse CD2 or mouse CD48, the relevant cDNA fragments were amplified by PCR and cloned into pSK-Fc, which also

encodes the Fc portion of human IgG1. Subsequently, fusion constructs were cloned into pXM139 for transient expression in Cos-1 cells. For production of the Fc fusion proteins encompassing the extracellular domain of human CD2, human CD48, or human CD58, the appropriate cDNA fragments were amplified by PCR and cloned into phIgG1-Fc, which also encodes the Fc portion of human IgG1, for transient expression in HEK293T cells. Fc fusion proteins were purified from supernatants using rProtein A Sepharose Fast Flow (MilliporeSigma, GE 17-1279-03).

Antibodies

For flow cytometry, the following mAbs were used. Anti-CD62L (MEL-14), anti-CD44 (1 M7), anti-MHC class I, H-2Kb (AF6-88.5.5.3), anti-CD25 (PC61.5), anti-Foxp3 (NRRF-30), and anti- MHC class I, H-2Kd (SF1-1.1.1) were purchased from eBioscience (San Diego, CA, USA). Anti-human CD2 (RPA-2.10), anti-human CD48 (BJ40), anti-human CD58 (TS2/9), anti-human TCRa/b (IP26), anti-human CD3 (UCHT1), anti-human CD45 (HI30), anti-TCR Va2 (B20.1), anti-CD8a (53-6.7), anti-CD3e (145-2C11), anti-TCRb (H57-597), anti-CD107a (1D4B), anti-NK1.1 (PK136), anti-CD2 (RM2-5), anti-CD48 (HM48-1), anti-2B4 [m2B4 (B6) 458.1], anti- CD4 (RM4-5), rat IgG2a k isotype control (RTK2758), mouse IgG1 k isotype control Ab (MOPC-21), Armenian hamster IgG isotype control Ab (HTK888), and rat IgG2b k isotype control (RTK4530) were from BioLegend (San Diego, CA, USA). Anti-TCR Vb8.1/8.2 (MR5-2) and anti-CD45 (30-F11) were from BD Biosciences (Mississauga, Ontario, Canada). For immunofluorescence, the fol-lowing mAbs were used: anti-CD2 RM2-5 (BD Biosciences) and anti-CD48 HM48-1 (BioLegend). For cell stimulation, the following mAbs were used: anti-CD3 145-2C11 (Thermo Fisher Scientific), anti-CD28 37.51 (Thermo Fisher Scientific), anti-TCRb H57-597 (BioLegend), anti-human TCRa/b IP26 (BioLegend), and anti- human CD3 OKT3 (Thermo Fisher Scientific). For blockade treat-ment in Figs. 1C and 2C, anti-CD2 RM2-5 (BioLegend) or isotype control was used. Anti–b-actin mAb C4, Abs recognizing Erk (catalog no. 06-182), and phospho-specific Abs recognizing phos-photyrosine (mAb 4G10) or pErk (pT202pY204; mAb E10) were obtained from Millipore (Billerica, MA), Cell Signaling Technology (Danvers, MA), or Santa Cruz Biotechnology Inc. (Santa Cruz, CA). Rabbit Ab against Lck was generated in our laboratory (37).

Functional assays using freshly purified T cells

Purified CD4+ or CD8+ splenic T cells (106 cells ml−1; unless speci-fied, 105 cells in 100 ml per well were used in all functional assays) from the indicated mice were stimulated with the indicated concentrations of anti-CD3 mAb 145-2C11 coated on plastic, with or with-out soluble anti-CD28 mAb 37.51 (1 mg ml−1), Con A (4 mg ml−1; Sigma-Aldrich), or PMA (100 ng ml−1; Sigma-Aldrich) plus ionomycin (1 mg ml−1; Sigma-Aldrich). For anti-CD2 Ab blockade experiments, assays were as usual except that rat anti-CD2 RM2-5 or isotype con-trol rat IgG2b G013B8 (1 mg ml−1, coated on plastic) was also added. For the alloreactivity assays, purified CD8+ T cells (106 cells ml−1) were incubated for 2 days with MHC-mismatched irradiated spleno-cytes (2500 rad) at the indicated effector-to-target (E:T) ratios. For stimulation with the superantigen SEB (Sigma-Aldrich, St. Louis, MO), CD4+ T cells (106 cells ml−1) were stimulated for 2 days with the indicated concentrations of SEB in the presence of irradiated splenocytes as APCs (38). For OT-I mice, CD8+ T cells (106 cells ml−1) were stimulated for 24 hours with the OVA-derived SIINFEKL (N4) agonist peptide or SIIGFEKL (G4) weak agonist peptide (0.01 to 1000 nM) in the presence of irradiated splenocytes as APCs. For OT-II mice, CD4+ T cells (106 cells ml−1) were stimulated for 2 days with the OVA peptide 323–339 (0.01 to 1000 nM) in the presence of irradiated splenocytes as APCs. All assays were done in triplicates. Proliferation was measured by monitoring [3H]thymidine incorpo-ration, whereas cytokine production was revealed by enzyme-linked immunosorbent assay (ELISA) (R&D Systems, Minneapolis, MN).

Cytotoxicity and assays with previously activated T cells

OT-I CD8+ T cells were primed for 36 hours with SIINFEKL peptide (20 mM) in the presence of irradiated splenocytes. They were subsequently expanded for 48 hours in medium containing IL-2 (50 U ml−1). Then, primed CD8+ T cells were incubated with APCs (EL-4 cells, RMA cells, or previously activated CD4+ T cells; 3000 cells per well in 96-well plate), which were previously labeled with 51Cr and pulsed or not for 1 hour with SIINFEKL peptide (1 mM). Cytotoxicity assays were then performed in duplicates at the indicated E:T ratios. Maximal 51Cr release and spontaneous release were de-termined by adding 1.0% (v/v) Triton X-100 or medium, respectively. Release of 51Cr into the supernatant was measured with a g-counter (PerkinElmer, Wallac Wizard 1470). For induction of CD107a surface exposure, assays were conducted in the presence of AF 647–conjugated anti-CD107a mAb 1D4B (BioLegend). After 4 hours, cells were stained with fluorescein isothiocyanate (FITC)–conjugated anti- CD8a mAb 53-6.7 (BioLegend) and analyzed using a BD LSR Fortessa flow cytometer (BD Biosciences). OT-I T cells were identi-fied by gating on CD8+ cells. Experiments with primed CD8+ T cells assessing proliferation or cytokine production were conducted using similar conditions.

Graft-versus-host disease

A 3:1 mixture of CD8+ T cells (1.8 × 106) and CD4+ T cells (0.6 × 106) from the indicated mice in the C57BL/6 background was injected intravenously into sublethally irradiated (5 Gy, gamma irradiator with a Cesium137 source) BALB/c mice. PBS was injected as control. Mice were then monitored every day for weight loss and survival. Mice exhibiting a body weight loss greater than 30% were immedi-ately euthanized, and their death was recorded as having occurred the next day. Otherwise, mice were sacrificed at the indicated times. The number and cell surface markers of donor cells in the spleen were determined using flow cytometry.

Binding to soluble Fc fusion protein

Previously activated OT-II mouse T cells or Jurkat human T cells were incubated for 30 min on ice with the indicated Fc fusion proteins, which all carry the Fc portion of human IgG1. Subsequently, cells were washed and stained with AF 647–conjugated F(ab')2 fragments of goat anti-human IgG for 30 min on ice. Fc binding was evaluated by flow cytometry. AF 647–labeled human IgG1 was used as control.

Immunofluorescence microscopy

To address the localization of CD2 and CD48, CD4+ T cells were activated with anti-CD3 mAb 145-2C11 (3 mg ml−1) and anti-CD28 mAb 37.51 (1 mg ml−1), expanded in IL-2–containing medium, and seeded onto poly-L-lysine (Sigma-Aldrich)–coated slides. After in-cubation for 15 min at 37°C in a cell culture incubator, unattached cells were removed by washing with PBS. Subsequently, cells were fixed in PBS containing 4% paraformaldehyde (PFA; Biotium). Samples were washed twice with PBS and blocked for 30 min in PBS con-taining 5% bovine serum albumin. Cells were then incubated for 1 hour with AF 647–coupled anti-CD48 mAb HM48-1 and Brilliant Violet 421–coupled anti-CD2 mAb RM2-5. Slides were washed and mounted with fluorescent mounting solution (Dako). Images were acquired using a laser scanning confocal microscope LSM-700 (Zeiss). For quantification of fluorescence, raw images were reconstructed by the Zeiss Zen software processing tool (Black Edition). Fluores-cence intensity (FI) profiles for Brilliant Violet 421 (CD2) and AF 647 (CD48) were determined along a solid line drawn on the images, using Zeiss Zen 2012 (Blue Edition). FI profiles along the solid line are represented by the curves.

FRET assay

The acceptor photobleaching FRET assay was performed as described (23). In essence, a SNAP tag or a CLIP tag was added to the N terminus of mouse CD48 or mouse CD2, respectively, using PCR. After

clon-ing into the vector pFB-Neo, constructs were cotransfected into HEK293T cells using polyethylenimine (Polysciences, 23966-1). After 48 hours, cells were harvested and seeded onto poly-L-lysine (Sigma-Aldrich, P8920)–treated 96-well plates with glass bottoms (MatTek Corporation, P35G-0-20-C). After 24 hours, cells were labeled with CLIP-Surface 547 (New England Biolabs, S9233S) and SNAP- Surface AF 647 (New England Biolabs, S9136S) for 45 min at 37°C, followed by three washes with PBS. In some cases, Abs (3 mg ml−1) were included. Cells were then fixed for 10 min at room temperature with 4% PFA (20 ml; Biotium, 22023) and used for the FRET assay. Images were acquired with an LSM700 confocal microscope (Zeiss) by exciting CLIP-Surface 547 (energy donor) at 543 nm and SNAP- Surface AF 647 (energy acceptor) at 635 nm. The FRET images were acquired using ImageJ (Fiji) with the AccPbFRET plugin, as described (39).

Mouse CD4+ T cell isolation and short-term expansion before AP-MS analysis

CD4+ T cells were isolated from pooled lymph nodes and spleens with the Dynabeads Untouched Mouse CD4+ T Cell Kits (Life Technologies) with a >95% purity. Purified CD4+ T cells were activated with plate-bound anti-CD3 (5 mg ml−1; 145-2C11) and soluble anti-CD28 (1 mg ml−1; 37-51) Abs. After 2 days of cul-ture, CD4+ T cells were grown for an additional 48 hours in the presence of IL-2 (5 to 10 U ml−1) before being used for AP-MS experiments.

Biochemical studies

To study TCR-triggered protein tyrosine phosphorylation or Erk activation, 10 × 106 freshly isolated CD4+ splenic T cells (in 100 ml of PBS) were stimulated for the indicated periods of time at 37°C with biotinylated anti-TCRb (5 mg ml−1) and avidin (10 mg ml−1). Unstimulated controls were incubated with avidin alone. Cells were then lysed by the addition of a twice-concentrated lysis buffer [100 mM tris (pH 7.5), 300 mM NaCl, 40 mM EDTA, and 2% n-dodecyl b-D-maltoside] supplemented with protease and phosphatase in-hibitors (18, 37, 38). After 15 min of incubation on ice, cell lysates were centrifuged at 14,000 rpm for 5 min at 4°C to remove the nuclei. Equivalent amounts of cellular proteins were then separated by 8% SDS–polyacrylamide gel electrophoresis and transferred to polyvinylidene difluoride membranes. After overnight incubation of the membranes with primary Abs at 4°C, proteins were visual-ized using a horseradish peroxidase–coupled secondary Ab and enhanced chemiluminescence (GE Health). Calcium fluxes were monitored by flow cytometry, as previously described (38). Briefly, purified CD4+ T cells or Jurkat cells (2.5× 106 cells ml−1) were loaded with the calcium indicator dye Indo-1 (Thermo Fisher Scientific) for 30 min at 37°C. After washing, they were stimulated at 37°C with biotinylated anti-mouse TCR mAb H57-597 (0.5 mg ml−1) or anti-human TCR mAb IP26 (1 mg ml−1) and avidin, Con A (4 mg ml−1), or PHA (10 mg ml−1; Sigma-Aldrich). For the mixing experiments, CD2 KO T cell (CD45.1) and CD48 KO T cell (CD45.2) were la-beled with anti-mouse CD45.1 and mixed at 1:1 ratio; mixed cells were then stimulated with Con A, anti-mouse TCR mAb H57-597, or ionomycin. Changes in intracellular calcium were monitored over time by a BD LSR Fortessa flow cytometer (BD Biosciences), using the UV450/UV530 fluorescence ratio. As control, cells were stimulated with the calcium ionophore ionomycin (1 mg ml−1; Sigma-Aldrich). For peptide pull-down assays, synthetic biotinylated peptides (GenScript USA Inc., Piscataway, NJ) corresponding to the various proline-rich sequences of WT mouse CD2 were immo-bilized on avidin beads (Neutravidin, Thermo Fisher Scientific). The following peptides were used: M1, VALQAPPPPGHHLQ; M2, HHLQTPGHRPLPPGHRTR; M3, QQKKRPPPSGTQI; M4, HQQKGPPLPRPRVQPK; M5, RPRVQPKPPCGSGD. Immobilized peptides were then incubated for 1.5 hours at 4°C with postnuclear lysates (2 mg per sample) of splenic CD4+ T cells preactivated with anti-CD3 (3 mg ml−1) plus anti-CD28 (1 mg ml−1) Abs. Samples were then processed for immunoblotting with anti-Lck Abs.

Statistical analyses

GraphPad Prism software was used for all statistical analyses. Statis-tics were obtained using unpaired Student's t test (two-tailed). For survival analyses, a log-rank (Mantel-Cox) test was performed (35). Data shown are means ± SD.

REFERENCES AND NOTES

1. A. K. Chakraborty, A. Weiss, Insights into the initiation of TCR signaling. Nat. Immunol. 15, 798–807 (2014).

2. A. C. Chan, D. M. Desai, A. Weiss, The role of protein tyrosine kinases and protein tyrosine phosphatases in T cell antigen receptor signal transduction. Annu. Rev. Immunol. 12, 555–592 (1994).

3. A. Veillette, S. Latour, D. Davidson, Negative regulation of immunoreceptor signaling. Annu. Rev. Immunol. 20, 669–707 (2002).

4. S. L. McArdel, C. Terhorst, A. H. Sharpe, Roles of CD48 in regulating immunity and tolerance. Clin. Immunol. 164, 10–20 (2016).

5. A. H. Sharpe, Analysis of lymphocyte costimulation in vivo using transgenic and 'knockout' mice. Curr. Opin. Immunol. 7, 389–395 (1995).

6. M. L. Dustin, T. A. Springer, Role of lymphocyte adhesion receptors in transient interactions and cell locomotion. Annu. Rev. Immunol. 9, 27–66 (1991).

7. N. Wu, A. Veillette, SLAM family receptors in normal immunity and immune pathologies. Curr. Opin. Immunol. 38, 45–51 (2016).

8. P. Demetriou, E. Abu-Shah, S. Valvo, S. McCuaig, V. Mayya, A. Kvalvaag, T. Starkey,

K. Korobchevskaya, L. Y. W. Lee, M. Friedrich, E. Mann, M. A. Kutuzov, M. Morotti, N. Wietek, H. Rada, S. Yusuf, J. Afrose, A. Siokis; Oxford IBD Cohort Investigators, P. Allan, T. Ambrose, C. Arancibia, A. Bailey, E. Barnes, E. Bird-Lieberman, J. Bornschein, O. Brain, B. Braden, J. Collier, J. Cobbold, E. Culver, J. East, L. Howarth, P. Klenerman, S. Leedham, R. Palmer, M. Pavlides, F. Powrie, A. Rodrigues, J. Satsangi, A. Simmons, P. Sullivan, H. Uhlig, A. Walsh, M. Meyer-Hermann, A. A. Ahmed, D. Depoil, M. L. Dustin, A dynamic CD2-rich compartment at the outer edge of the immunological synapse boosts and integrates signals. Nat. Immunol. 21, 1232–1243 (2020).

9. K. H. Lee, A. R. Dinner, C. Tu, G. Campi, S. Raychaudhuri, R. Varma, T. N. Sims, W. R. Burack,

H. Wu, J. Wang, O. Kanagawa, M. Markiewicz, P. M. Allen, M. L. Dustin, A. K. Chakraborty, A. S. Shaw, The immunological synapse balances T cell receptor signaling and degradation. Science 302, 1218–1222 (2003).

10. V. Zurli, T. Montecchi, R. Heilig, I. Poschke, M. Volkmar, G. Wimmer, G. Boncompagni, G. Turacchio, M. M. D'Elios, G. Campoccia, N. Resta, R. Offringa, R. Fischer, O. Acuto, C. T. Baldari, A. Kabanova, Phosphoproteomics of CD2 signaling reveals AMPK-dependent regulation of lytic granule polarization in cytotoxic T cells. Sci. Signal. 13, eaaz1965 (2020).

11. C. Binder, F. Sellberg, F. Cvetkovski, E. Berglund, D. Berglund, Siplizumab, an anti-CD2 monoclonal antibody, induces a unique set of immune modulatory effects compared to alemtuzumab and rabbit anti-thymocyte globulin in vitro. Front. Immunol. 11, 592553 (2020).

12. N. Killeen, S. G. Stuart, D. R. Littman, Development and function of T cells in mice with a disrupted CD2 gene. EMBO J. 11, 4329–4336 (1992).

13. M. F. Bachmann, M. Barner, M. Kopf, CD2 sets quantitative thresholds in T cell activation. J. Exp. Med. 190, 1383–1392 (1999).

14. S. J. Teh, N. Killeen, A. Tarakhovsky, D. R. Littman, H. S. Teh, CD2 regulates the positive selection and function of antigen-specific CD4− CD8+ T cells. Blood 89, 1308–1318 (1997).

15. J. M. Green, V. Karpitskiy, S. L. Kimzey, A. S. Shaw, Coordinate regulation of T cell activation by CD2 and CD28. J. Immunol. 164, 3591–3595 (2000).

16. A. J. Kaplan, K. D. Chavin, H. Yagita, M. S. Sandrin, L. H. Qin, J. Lin, G. Lindenmayer, J. S. Bromberg, Production and characterization of soluble and transmembrane murine CD2. Demonstration that CD48 is a ligand for CD2 and that CD48 adhesion is regulated by CD2. J. Immunol. 151, 4022–4032 (1993).

17. A. Muhammad, H. B. Schiller, F. Forster, P. Eckerstorfer, R. Geyeregger, V. Leksa, G. J. Zlabinger, M. Sibilia, A. Sonnleitner, W. Paster, H. Stockinger, Sequential cooperation of CD2 and CD48 in the buildup of the early TCR signalosome. J. Immunol. 182, 7672–7680 (2009).

18. D. Davidson, M. C. Zhong, P. P. Pandolfi, S. Bolland, R. J. Xavier, B. Seed, X. Li, H. Gu, A. Veillette, The Csk-associated adaptor PAG inhibits effector T cell activation in cooperation with phosphatase PTPN22 and Dok adaptors. Cell Rep. 17, 2776–2788 (2016).

19. J. L. Stolfi, C. C. Pai, W. J. Murphy, Preclinical modeling of hematopoietic stem cell transplantation - advantages and limitations. FEBS J. 283, 1595–1606 (2016).

20. G. Voisinne, K. Kersse, K. Chaoui, L. Lu, J. Chaix, L. Zhang, M. G. Menoita, L. Girard, Y. Ounoughene, H. Wang, O. Burlet-Schiltz, H. Luche, F. Fiore, M. Malissen, A. G. de Peredo, Y. Liang, R. Roncagalli, B. Malissen, Quantitative interactomics in primary T cells unveils TCR signal diversification extent and dynamics. Nat. Immunol. 20, 1530–1541 (2019).

21. J. Celis-Gutierrez, P. Blattmann, Y. Zhai, N. Jarmuzynski, K. Ruminski, C. Grégoire, Y. Ounoughene, F. Fiore, R. Aebersold, R. Roncagalli, M. Gstaiger, B. Malissen, Quantitative interactomics in primary T cells provides a rationale for concomitant PD-1 and BTLA coinhibitor blockade in cancer immunotherapy. Cell Rep. 27, 3315–3330.e7 (2019).

22. A. R. Arulanandam, P. Moingeon, M. F. Concino, M. A. Recny, K. Kato, H. Yagita, S. Koyasu, E. L. Reinherz, A soluble multimeric recombinant CD2 protein identifies CD48 as a low affinity ligand for human CD2: Divergence of CD2 ligands during the evolution of humans and mice. J. Exp. Med. 177, 1439–1450 (1993).

23. Y. Zhao, D. L. Harrison, Y. Song, J. Ji, J. Huang, E. Hui, Antigen-presenting cell-intrinsic PD-1 neutralizes PD-L1 in cis to attenuate PD-1 signaling in T cells. Cell Rep. 24, 379–390. e6 (2018).

24. A. K. Mitra, H. Célia, G. Ren, J. G. Luz, I. A. Wilson, L. Teyton, Supine orientation of a murine MHC class I molecule on the membrane bilayer. Curr. Biol. 14, 718–724 (2004).

25. A. D. Douglass, R. D. Vale, Single-molecule microscopy reveals plasma membrane microdomains created by protein-protein networks that exclude or trap signaling molecules in T cells. Cell 121, 937–950 (2005).

26. M. L. Hermiston, Z. Xu, A. Weiss, CD45: A critical regulator of signaling thresholds in immune cells. Annu. Rev. Immunol. 21, 107–137 (2003).

27. Z. Dong, A. Veillette, How do SAP family deficiencies compromise immunity? Trends Immunol. 31, 295–302 (2010).

28. J. Back, E. L. Malchiodi, S. Cho, L. Scarpellino, P. Schneider, M. C. Kerzic, R. A. Mariuzza, W. Held, Distinct conformations of Ly49 natural killer cell receptors mediate MHC class I recognition in trans and cis. Immunity 31, 598–608 (2009).

29. Y. Liu, M. A. Cuendet, L. Goffin, R. Šachl, M. Cebecauer, L. Cariolato, P. Guillaume, P. Reichenbach, M. Irving, G. Coukos, I. F. Luescher, CD8 binding of MHC-peptide complexes in cis or trans regulates CD8+ T-cell responses. J. Mol. Biol. 431, 4941–4958 (2019).

30. M. R. Junttila, S. Saarinen, T. Schmidt, J. Kast, J. Westermarck, Single-step Strep-tag purification for the isolation and identification of protein complexes from mammalian cells. Proteomics 5, 1199–1203 (2005).

31. R. Roncagalli, S. Hauri, F. Fiore, Y. Liang, Z. Chen, A. Sansoni, K. Kanduri, R. Joly, A. Malzac, H. Lähdesmäki, R. Lahesmaa, S. Yamasaki, T. Saito, M. Malissen, R. Aebersold, M. Gstaiger, B. Malissen, Quantitative proteomics analysis of signalosome dynamics in primary T cells identifies the surface receptor CD6 as a Lat adaptor-independent TCR signaling hub. Nat. Immunol. 15, 384–392 (2014).

32. P. Soriano, The PDGF alpha receptor is required for neural crest cell development and for normal patterning of the somites. Development 124, 2691–2700 (1997).

33. S. J. Pettitt, Q. Liang, X. Y. Rairdan, J. L. Moran, H. M. Prosser, D. R. Beier, K. C. Lloyd, A. Bradley, W. C. Skarnes, Agouti C57BL/6N embryonic stem cells for mouse genetic resources. Nat. Methods 6, 493–495 (2009).

34. Z. Dong, D. Davidson, L. A. Pérez-Quintero, T. Kurosaki, W. Swat, A. Veillette, The adaptor SAP controls NK cell activation by regulating the enzymes Vav-1 and SHIP-1 and by enhancing conjugates with target cells. Immunity 36, 974–985 (2012).

35. Z. Dong, M. E. Cruz-Munoz, M. C. Zhong, R. Chen, S. Latour, A. Veillette, Essential function for SAP family adaptors in the surveillance of hematopoietic cells by natural killer cells. Nat. Immunol. 10, 973–980 (2009).

36. H. Guo, S. A. Cranert, Y. Lu, M. C. Zhong, S. Zhang, J. Chen, R. Li, S. E. Mahl, N. Wu, D. Davidson, S. N. Waggoner, A. Veillette, Deletion of Slam locus in mice reveals inhibitory role of SLAM family in NK cell responses regulated by cytokines and LFA-1. J. Exp. Med. 213, 2187–2207 (2016).

37. D. Davidson, X. Shi, M. C. Zhong, I. Rhee, A. Veillette, The phosphatase PTP-PEST promotes secondary T cell responses by dephosphorylating the protein tyrosine kinase Pyk2. Immunity 33, 167–180 (2010).

38. D. Davidson, B. Schraven, A. Veillette, PAG-associated FynT regulates calcium signaling and promotes anergy in T lymphocytes. Mol. Cell. Biol. 27, 1960–1973 (2007).

39. J. Roszik, J. Szollosi, G. Vereb, AccPbFRET: An ImageJ plugin for semi-automatic, fully corrected analysis of acceptor photobleaching FRET images. BMC Bioinformatics 9, 346 (2008).

Acknowledgments: We thank members of the Veillette laboratory and Guillaume Voisinne of the Malissen laboratory for useful discussions and advice and M. Camus and E. Bouscasse at the IPBS proteomics facility (Toulouse) for technical help in mass spectrometry analysis. We thank Frédéric Fiore (CIPHE) for supervising the construction of the knock-in mice. Funding: This work was supported by grants from the Canadian Institutes of Health Research (MT-14429, MOP-82906, and FDN-143338) and the Terry Fox Research Institute (-22) to A.V. and from the Centre National de la Recherche Scientifique, the Institut National de la Santé et de la Recherche Médicale, the SUPER-BASILIC Project (ANR-AAP-2018 to B.M.), the Investissement d'Avenir program PHENOMIN (French National Infrastructure for mouse Phenogenomics; ANR-10-INBS-07, to B.M.), and the Agence Nationale de la Recherche (Investissement d'Avenir program of the French Ministry of Research, ProFI, Proteomics

French Infrastructure, ANR-10-INBS-08). B.L. held a Scholarship from the Chinese Science Council. A.V. holds the Canada Research Chair on Signaling in the Immune System.